Endogenous viral element-derived piRNAs are not required for production of ping-pong-dependent piRNAs from Diaphorina citri densovirus

Jared C. Nigg[1], Yen-Wen Kuo, and Bryce W. Falk

Department of Plant Pathology, University of California, 1 Shields Avenue, Davis, CA 95616

[1] Present address: Viruses and RNA Interference Unit, Institut Pasteur, UMR3569, CNRS, Paris, France

Abstract

Partial integrations of DNA and non-retroviral RNA virus genomes, termed endogenous viral elements (EVEs), are abundant in arthropod genomes and often produce PIWI-interacting RNAs (piRNAs) speculated to target cognate viruses through the ping-pong cycle, a post-transcriptional RNA silencing mechanism. Here we describe a Diaphorina citri densovirus (DcDV)-derived EVE in the genome of *Diaphorina citri*. We found that this EVE gives rise to DcDV-specific primary piRNAs and is unevenly distributed among *D. citri* populations. Unexpectedly, we found that DcDV is targeted by ping-pong-dependent viral piRNAs (vpiRNAs) in *D. citri* lacking the DcDV-derived EVE, while four naturally infecting RNA viruses of *D. citri* are not targeted by vpiRNAs. Furthermore, a recombinant Cricket paralysis virus containing a portion of the DcDV genome corresponding to the DcDV-derived EVE was not targeted by vpiRNAs during infection in *D. citri* harboring the EVE. These results represent the first report of ping-pong-dependent vpiRNAs outside of mosquitoes.

Introduction

24 The Piwi-interacting RNA (piRNA) pathway is a small RNA (sRNA) guided gene silencing
25 mechanism responsible for repressing transposable elements (TEs) in animals and emerging
26 evidence supports a role for this pathway in antiviral responses in some mosquito species and
27 mosquito-derived cell lines (1–5). In *Drosophila melanogaster*, biogenesis of primary piRNAs
28 begins with transcription of single-stranded piRNA precursor transcripts from discrete genomic
29 regions called piRNA clusters (6). TE sequences integrated into piRNA clusters can become
30 transcribed as part of a piRNA precursor transcript and these precursor transcripts are processed
31 into primary piRNAs that direct transcriptional and post-transcriptional silencing of TEs by
32 association with the Piwi-family Argonaute proteins Piwi and Aubergine, respectively (1).
33 During the ping-pong cycle, cleavage of sense TE RNA directed by Aubergine-bound antisense
34 primary piRNAs triggers production of sense secondary piRNAs from cleaved TE RNA and, in
35 turn, sense secondary piRNAs direct cleavage of antisense piRNA precursor transcripts via
36 association with another Piwi-family Argonaute protein, Argonaute 3 (Ago3), to specifically
37 amplify the response against active TEs (6). piRNAs are distinguished from other sRNAs by
38 their size (24-32 nt), nucleotide biases (uridine as the first nucleotide for primary piRNAs and
39 adenine as the tenth nucleotide for secondary piRNAs, known as the 1U and 10A bias), and
40 association with a Piwi-family Argonaute protein (1). Additionally, complementary piRNAs
41 produced by the ping-pong cycle have 5' ends separated by exactly 10 nt, known as the ping-
42 pong signature (1).
43
44 The presence of ping-pong-dependent virus-derived piRNAs (vpiRNAs) during infection with
45 several RNA viruses in *Aedes* and *Culex* mosquitoes and cell lines has been reported (2–5,7–12)
46 and reduced expression of piRNA pathway components leads to increased replication of Semliki

47 Forest virus, Bunyamwera virus, Cache Valley virus, and Rift Valley Fever virus in *Aedes*
48 *aegypti*-derived Aag2 cells (2–5). Despite the prevalence of virus-derived piRNAs and evidence
49 supporting their antiviral role, little is known regarding their biogenesis or antiviral function *in*
50 *vivo*. *Ae. aegypti* expresses an expanded group of Piwi-family Argonaute proteins containing
51 eight proteins (Piwi1-7 and Ago3) rather than the three proteins seen in *D. melanogaster* (Piwi,
52 Aub, and Ago3) (13). In Aag2 cells, Piwi5 and Ago3 are the primary Piwi-family Argonaute
53 proteins required for biogenesis of vpiRNAs upon infection with Sindbis virus (9). Importantly,
54 induction of the ping-pong cycle in mosquitoes is thought to involve recognition of exogenous
55 viral RNA, triggering biogenesis of primary vpiRNAs directly from viral RNA without the need
56 for primary piRNAs derived from endogenous loci (9,11). This is in contrast to the canonical
57 ping-pong cycle, which produces primary piRNAs only from endogenous transcripts (6). Thus,
58 mosquitoes possess a unique piRNA pathway that produces vpiRNAs by virtue of novel
59 functionality that has so far not been found in other groups of organisms. Indeed, the piRNA
60 pathway was not found to play an antiviral role in *D. melanogaster* and no evidence for an
61 antiviral piRNA pathway, or even the presence of ping-pong-dependent vpiRNAs, has been
62 reported outside of the mosquito lineage (14).
63
64 Arthropod genomes contain an abundance of sequences derived from DNA viruses and non-
65 retroviral RNA viruses (15–20) . These sequences, termed endogenous viral elements (EVEs),
66 are often enriched within piRNA clusters and are known to serve as sources of primary piRNAs
67 in a wide variety of arthropod species (15–17). These observations have led to speculation that
68 EVE-derived primary piRNAs may play an antiviral role by targeting cognate viruses in a
69 manner analogous to piRNA-mediated repression of TEs via the ping-pong cycle (15–17).

70 Importantly, such a role for EVE-derived piRNAs could theoretically be mediated by the
71 canonical ping-pong cycle and could thus expand the antiviral potential of the piRNA pathway
72 beyond mosquitoes. In support of this idea, Whitfield et al. found that a single EVE-derived
73 piRNA maps to the genome of Phasi Charoen-like virus (PCLV) in Aag2 cells, which are
74 persistently infected with PCLV, and that a vpiRNA is produced from the complementary strand
75 (16). Moreover, the authors found that knockdown of Piwi4 led to a ~2 fold increase in the
76 abundance of PCLV RNA in Aag2 cells (16). While these results are intriguing, it is difficult to
77 assess how the EVE-derived piRNA affects PCLV RNA abundance in the context of the Piwi4
78 knockdown, as only global sRNA mapping data to the entire PCLV nucleocapsid-encoding
79 segment are presented, the abundance of the EVE-derived piRNA and its potential PCLV-
80 derived ping-pong partner were not discussed, and Piwi4 knockdown has been shown to reduce
81 both siRNA and piRNA production (16,21). More recently, Tassetto et al. found that Piwi4 is
82 required for vpiRNA maturation in Aag2 cells and binds specifically to piRNAs derived from
83 EVEs (21). Furthermore, they found that insertion of EVE sequences into the 3' UTR of Sindbis
84 virus reduced viral replication in a Piwi4-dependent manner in Aag2 cells (21). These results
85 raise the possibility that EVE-derived piRNAs may target cognate viruses in these cells through
86 an interaction with Piwi4, however, detailed sRNA profiles and more thorough examinations of
87 the interplay between virus-specific piRNAs derived from endogenous and exogenous sources
88 are needed to establish the link between EVE-derived piRNAs and an antiviral response.
89
90 We previously identified the EVEs present within the genomes of 48 arthropod species (15).
91 Among the EVEs that we estimated to be similar enough to their corresponding exogenous
92 viruses at the nucleotide level such that piRNAs derived from them could potentially target viral

93 RNA during infection, Diaphorina citri densovirus (DcDV) and a DcDV-derived EVE located
94 within a piRNA cluster on *Diaphorina citri* genomic scaffold 2850 stood out as an EVE-virus
95 pair sharing exceptionally high nucleotide identity over a relatively long region (15). *D. citri*,
96 also known as the Asian citrus psyllid, is a hemipteran insect pest and serves as a vector of
97 *Candidatus* Liberibacter species that cause Huanglongbing, or citrus greening disease, in all
98 types of commercially cultivated citrus throughout the world (22). This disease represents the
99 greatest threat to the citrus industry worldwide and has devastated many citrus growing regions,
100 such as in the US state of Florida, where citrus production has decreased by 74% since the first
101 report of citrus greening disease in the state in 2005 (23). Control strategies for the disease are
102 limited and primarily involve removal of infected trees and management of *D. citri* populations
103 with chemical insecticides (24). The continued spread of citrus greening disease and the
104 development of insecticide resistance in field populations of *D. citri* highlight the need for new
105 management approaches (24). Biological control strategies relying on infectious agents have
106 proven to be effective methods for controlling insect pests and the use of parasites and viruses
107 have been proposed as possible vector control approaches for *D. citri* (25–28). Current
108 understanding of immune processes in *D. citri* is limited and studies in this field are needed to
109 facilitate the development of effective biological control strategies. In particular, antiviral
110 mechanisms in *D. citri* have not been experimentally evaluated. The presence of a highly similar
111 virus-EVE pair, a lack of novel Piwi-family of Argonaute proteins like those observed in
112 mosquitoes, and the need to study antiviral mechanisms in *D. citri* make this species an excellent
113 and relevant model to study the interactions between EVE-derived piRNAs and corresponding
114 viruses.
115

116 Here we further characterized the DcDV-derived EVE present within the *D. citri* genome. We
117 found that piRNAs are produced from this EVE in multiple tissue types and that this EVE is
118 conserved among some geographically distinct populations of *D. citri*, but is absent from other
119 populations. By analyzing sRNA profiles in *D. citri* insects infected with DcDV, we found that
120 this virus is targeted by ping-pong-dependent vpiRNAs independent of DcDV-derived EVEs and
121 endogenous DcDV-specific piRNAs. Additionally, analysis of sRNA profiles during infection
122 with other viruses suggests that RNA viruses are not a target of vpiRNAs in *D. citri*.
123
124
125 **Results**
126 *A DcDV-derived EVE with high nucleotide identity to DcDV is conserved in some populations*
127 *of D. citri, but absent in others*
128 We previously identified a 621 bp DcDV-derived EVE located within a piRNA cluster on *D.*
129 *citri* genomic scaffold 2850 by comparing deduced virus protein sequences to deduced *D. citri*
130 genome-encoded protein sequences using BLASTx (15). This EVE was 85.5% identical to the
131 corresponding region of the DcDV genome at the deduced amino acid level and resided just
132 downstream from another 624 bp EVE derived from a different portion of the DcDV genome. To
133 characterize these EVEs at the nucleotide level, we aligned the nucleotide sequence of the DcDV
134 genome to the region of the *D. citri* genome harboring these DcDV-derived EVEs. We found
135 that this region of the *D. citri* genome contains sequences corresponding to the DcDV inverted
136 terminal repeats (ITRs) and to two regions of the non-structural protein (NS) gene cassette
137 together spanning 1,396 bp. For simplicity we refer to these regions as endogenous ITR (EITR)
138 and endogenous NS (ENS) (Fig. 1a). Notably, the portion of ENS spanning nucleotides 7,523 to

139 8,175 within genomic scaffold 2850 shares 86% nucleotide identity with the corresponding
140 region of the DcDV genome.
141
142 Because our EVE prediction shown in Fig. 1a was based only on BLAST results and a previous
143 *D. citri* genome assembly, we wanted to confirm the presence, sequence, and organization of the
144 DcDV-derived EVEs. To confirm the presence of these EVEs, we designed PCR primers to
145 amplify this region from *D. citri* genomic DNA (Fig. 1a). We obtained PCR products of
146 unexpected size (based on the available sequence of scaffold 2850 and the organization depicted
147 in Fig. 1a) for both primer sets (Fig. 1b). Sequencing of these PCR products revealed that the
148 portion of ENS spanning nucleotides 5,248 to 5,871 within genomic scaffold 2850 was not
149 present and the distance between the ITR-like fragments was 3,885 bp rather than 11,038 bp.
150 Additionally, EITR was 210 bp instead of 114 bp. The portion of ENS corresponding to the
151 region between DcDV nucleotides 263-916 was present and closely matched the sequence
152 observed by BLAST. Figure 1c shows the correct organization of this region of the DcDV
153 genome, as confirmed by sequencing of the PCR products shown in Fig. 1b. This organization
154 and sequence is supported by a more recent draft of the *D. citri* genome assembled using PacBio
155 long reads (Diaci2.0,
156 ftp://ftp.citrusgreening.org/genomes/Diaphorina_citri/assembly/DIACI_v2.0/).
157
158 Our PCR reactions were performed using DNA extracted from *D. citri* insects collected from a
159 colony located at the University of California Davis Contained Research Facility (CRF) that was
160 originally started using insects collected in the US state of California (this colony is designated
161 CRF-CA). The *D. citri* reference genome used for BLAST searches and nucleotide alignments

162 was produced by sequencing DNA from insects collected in the US state of Florida (29).
163 Haplotype network analysis of global *D. citri* populations based on the mitochondrial
164 cytochrome oxidase subunit I gene indicates the existence of 44 *D. citri* haplotypes belonging to
165 two distinct lineages, denoted lineages A and B (30–32). The invasion history of *D. citri* out of
166 Southern Asia has resulted in segregation of the two lineages, such that only lineage B is found
167 in North America, while lineage A predominates in Southeast Asia, Africa, and South America
168 (30). Besides CRF-CA, three other *D. citri* colonies are maintained at the CRF and these were
169 started using *D. citri* insects collected in Taiwan, Uruguay, and the US state of Hawaii
170 (designated CRF-TW, CRF-Uru, and CRF-HI, respectively). To determine whether ENS is
171 conserved among geographically distinct *D. citri* populations, we performed PCR using primers
172 flanking ENS and DNA extracted from insects collected from CRF-CA, CRF-TW, CRF-Uru,
173 and CRF-HI. We also included DNA extracted from field collected *D. citri* insects from
174 Pakistan, Brazil, and the US states of Arizona and Florida. We obtained nearly identical PCR
175 products from insects from CRF-CA, CRF-HI, Pakistan, Arizona, and Florida, but no PCR
176 products from insects from CRF-TW, CRF-Uru, or Brazil (Fig. 2a & S1). Based on the known
177 distribution of the two *D. citri* lineages, these results suggest that ENS is absent in *D. citri* from
178 lineage A.
179
180 Sequences derived from some insect infecting viruses are maintained as circular episomal
181 molecules that produce virus-specific sRNAs (12,33). Given the heterogenous distribution of
182 ENS among *D. citri* populations, we examined whether ENS is maintained episomally rather
183 than representing a true EVE. When we performed a Southern blot with DNA extracted from
184 CRF-CA *D. citri* using an RNA probe based on the sequence of ENS we observed a single DNA

185 species at high molecular weight (>12,000 bp) from undigested DNA and two species of lower
186 molecular weight in DNA digested with PstI and HindIII, indicating that ENS resides in high
187 molecular weight genomic DNA rather than low molecular weight episomal DNA (Fig. 2b). The
188 observation of two DNA species in the digested sample does not represent a second DcDV-like
189 EVE because ENS contains a PstI clevage site. To confirm that ENS is a true EVE, we treated *D.*
190 *citri* genomic DNA with an exonuclease to remove genomic DNA, but not circular episomal
191 DNA, and performed PCR with ENS-specific primers using exonuclease-treated DNA as
192 template. We obtained a PCR product from non-digested DNA, but not from digested DNA (Fig.
193 2c). Together, these results indicate the ENS is indeed integrated into the *D. citri* genome.
194 Finally, strand specific RT-PCR indicates that ENS is bidirectionally transcribed, although the
195 majority of transcripts are antisense to the corresponding DcDV transcript (Fig. 2d).
196
197
198 *ENS and EITR give rise to DcDV-specific primary piRNAs*
199 To evaluate whether ENS and EITR give rise to virus-specific primary piRNAs as described for
200 other EVEs, we mapped sRNAs from CRF-CA *D. citri* not infected with DcDV to the DcDV
201 genome. We found that sRNAs purified from CRF-CA *D. citri* mapped to EITR and to the
202 negative strand within the portion of the DcDV genome corresponding to ENS (i.e. antisense to
203 DcDV transcripts), but not to other regions (Fig. 3a). The size of these sRNAs was characteristic
204 of piRNAs and they possessed a strong 1U bias (Fig. 3b & c). Similar results were obtained for
205 other *D. citri* populations that are not infected with DcDV and for which sRNA datasets are
206 available (Fig. S2a & b). As expected based on the lack of ENS in *D. citri* insects collected in
207 Brazil or from CRF-Uru, DcDV-specific piRNAs were not observed in these insects (Fig. S2c &

208 d). We note that the DcDV ITRs are comprised of a 210 nt hairpin present on both ends of the
209 DcDV genome. Thus, it is not possible to determine whether the sRNAs mapping to EITR are
210 specific to the positive or the negative strand. For this reason, because of the relatively small size
211 of EITR compared to ENS, and because EITR does not correspond to a transcribed region of the
212 DcDV genome (34), we chose to focus our analysis on piRNAs derived from ENS.
213
214 The expression of piRNAs is known to display tissue specificity and piRNA expression patterns
215 could have important consequences for the ability of EVE-derived piRNAs to target cognate
216 viruses. To determine the tissue specificity of piRNAs produced from ENS and to determine the
217 tissues in which the ping-pong cycle is active in *D. citri*, we sequenced sRNAs purified from
218 dissected *D. citri* guts, heads, ovaries, testis, and hemolymph using insects collected from CRF-
219 CA. We found that while DcDV-specific piRNAs derived from ENS were present in all tissues
220 analyzed, their expression was significantly higher in *D. citri* guts than in any other tissue (Fig.
221 3d). The ping-pong cycle is restricted to germline tissues in *D. melanogaster* (1), however a
222 comprehensive analysis of somatic sRNAs mapping to TEs genome wide in 20 arthropod species
223 in combination with ancestral state reconstruction indicates that somatic ping-pong amplification
224 is widespread throughout arthropods despite having been independently lost in some species,
225 including *D. melanogaster* (35). To determine the tissues in which the ping-pong cycle is active
226 in *D. citri* we mapped sRNAs from CRF-CA *D. citri* guts, heads, hemolymph, ovaries, and testis
227 to all TEs identified within the *D. citri* genome and analyzed the mapped 27-32 nt sRNAs for the
228 presence of ping-pong signatures. We found evidence for ping-pong amplification of TE-derived
229 piRNAs in all tissues examined (Fig. S3).
230

231

232 *DcDV is targeted by ping-pong-dependent piRNAs in the absence of a DcDV-derived EVE*

233 We previously found that *D. citri* from CRF-CA are resistant to infection with DcDV (34). In
234 contrast, the virus is maintained as a persistent, maternally transmitted infection in *D. citri* from
235 CRF-TW (34). Thus, to understand the sRNA-based response to DcDV infection in *D. citri*, we
236 sequenced sRNAs from DcDV-infected *D. citri* from CRF-TW. These results revealed a major
237 population of 21 nt sRNAs, indicative of an siRNA-based response (Fig. 4a). Unexpectedly, we
238 also observed a smaller peak within the piRNA size range centered at 29 nt and we obtained
239 99.5% coverage of transcribed regions of the DcDV genome by mapping only 27-32 nt sRNAs
240 (Fig. 4a & b). We found that complementary 27-32 nt sRNAs mapping to opposite strands
241 throughout the DcDV genome possessed 5' ends separated by 10 nt more often than expected by
242 chance, an indication of ping-pong amplification (Z-score = 4.05±0.08)(Fig. 4c). Moreover, we
243 detected the 1U and 10A biases typical of ping-pong amplification in 27-32 nt sRNAs mapping
244 antisense and sense to the canonical DcDV transcripts, respectively (Fig. 4d & e).

245

246 We found that ENS is not present in the genome of CRF-TW *D. citri* (Fig. 2a), thus our
247 observation of ping-pong-dependent DcDV-derived piRNAs in these insects suggests that DcDV
248 is targeted by piRNAs independent of ENS. However, because this result was obtained by
249 performing PCR using primers flanking ENS, it is possible that ENS is present in CRF-TW *D.*
250 *citri,* but resides in different genomic context than seen in other *D. citri* populations. ENS is not
251 identical to the corresponding region of the DcDV genome at the nucleotide level (Fig. 1c).
252 Thus, some piRNAs derived from ENS do not perfectly map to DcDV, providing a means with
253 which to distinguish some ENS-derived piRNAs from DcDV-derived piRNAs. To rule out the

254 possibility that ENS is present in the genome of CRF-TW *D. citri*, we mapped 27-32 nt sRNAs
255 from CRF-TW *D. citri* to the DcDV genome without allowing any mismatches. When the
256 unmapped reads from this analysis were mapped to ENS without allowing any mismatches, no
257 reads mapped. In contrast, we obtained an average of 55.8% coverage of the ENS sequence when
258 the same analysis was performed using sRNAs from CRF-CA *D. citri* (data not shown). This
259 result indicates that ENS is indeed not present in the genome of CRF-TW *D. citri* and that the
260 targeting of DcDV by ping-pong-dependent vpiRNAs in these insects is independent of ENS-
261 derived piRNAs.
262
263 We cannot exclude the possibility that the genome of CRF-TW *D. citri* harbors a different
264 piRNA-producing DcDV-derived EVE. Because DcDV is maternally transmitted to 100% of the
265 progeny of CRF-TW females (34), it is not possible to determine the repertoire of endogenous
266 piRNAs in these insects in the absence of DcDV infection. Thus, we analyzed the sRNAs present
267 in *D. citri* from CRF-Uru, as these insects lack ENS and are not infected with DcDV (Fig. 2a).
268 We found that no DcDV-specific piRNAs are produced in uninfected CRF-Uru *D. citri*,
269 indicating that these insects do not harbor a piRNA-producing DcDV-derived EVE (Fig. S2d).
270 The absence of DcDV-specific piRNAs was not due to a lack of piRNAs in general, as we
271 detected abundant ping-pong-dependent TE-derived piRNAs in these insects (Fig. S4). In
272 contrast to *D. citri* from CRF-CA which are resistant to DcDV infection, we found that *D. citri*
273 from CRF-Uru were susceptible to DcDV infection by both oral acquisition and intrathoracic
274 injection (Fig. S5a & b)(34). Moreover, the progeny of CRF-Uru *D. citri* infected with DcDV
275 were also infected with the virus (Fig. S5c). Analysis of sRNAs from the progeny of CRF-Uru
276 *D. citri* that had been infected with DcDV by intrathoracic injection revealed the presence of

277 ping-pong-dependent DcDV-derived piRNAs (ping-pong Z-score = 2.55) (Fig. S6). Together,
278 these results demonstrate that DcDV is targeted by ping-pong-dependent vpiRNAs in two
279 populations of *D. citri* independent of EVE-derived piRNAs.
280
281
282 *Other viruses of D. citri are not targeted by piRNAs*
283 Besides DcDV, there are five other viruses known to infect *D. citri*: Diaphorina citri reovirus
284 (double-stranded RNA), Diaphorina citri picrona-like virus (plus strand single-stranded RNA; +
285 ssRNA), Diaphorina citri bunyavirus (minus strand single-stranded RNA), Diaphorina citri-
286 associated c virus (+ ssRNA), and Diaphorina citri flavi-like virus (+ ssRNA)(28,36–38). To
287 determine whether piRNAs are part of a general response to viruses in *D. citri*, we mapped
288 sRNAs from publicly available sRNA libraries known to be derived from insects infected with
289 one or more of each of these viruses to the corresponding viral genomes (with the exception of
290 Diaphorina citri-associated c virus for which no such sRNA library exists) (28,36). As expected,
291 we detected a prominent peak at 21 nt for each virus, indicating a siRNA-based response (Fig.
292 S7). While virus-derived sRNAs within the piRNA size range were present during infection with
293 all four viruses, there were no peaks above background levels within the piRNA size range and
294 27-32 nt reads lacked signatures typical of primary or ping-pong-dependent piRNAs (Fig. S7).
295 These results indicate that viruses in general are not targeted by piRNAs in *D. citri* and suggest
296 that the targeting of DcDV by the piRNA pathway in *D. citri* may be due to differences in the
297 infection cycles between RNA and DNA viruses.
298
299

300 *A recombinant CrPV-based reporter virus carrying DcDV sequence is not targeted by piRNAs in*
301 D. citri *that produce primary piRNAs from a DcDV-derived EVE*
302 As has been observed for RNA viruses in mosquitoes, our results suggest that DcDV is targeted
303 by ping-pong-dependent vpiRNAs due to the *de novo* production of vpiRNAs from exogenous
304 DcDV RNA. If EVE-derived piRNAs were to prime the ping-pong cycle in this context, it would
305 be difficult to distinguish priming driven by EVE-derived piRNAs from priming driven by virus-
306 derived vpiRNAs. Because our results suggest that RNA viruses are not targeted by vpiRNAs in
307 *D. citri*, we sought to construct a recombinant RNA virus harboring DcDV-derived EVE
308 sequence in order to study potential priming of the ping-pong cycle by EVE-derived piRNAs
309 without the background of vpiRNAs produced directly from viral RNA. For this purpose, we
310 used Cricket paralysis virus (CrPV), a dicistrovirus with a + ssRNA genome that was originally
311 isolated from field crickets (39). Due to the broad host range of CrPV and the availability of an
312 infectious clone, CrPV is often used to study antiviral mechanisms in insects (40,41).
313
314 To directly test the hypothesis that EVE-derived primary piRNAs can prime ping-pong
315 amplification during infection with viruses sharing complementary sequence, we inserted 57 nt
316 from the DcDV genome (from a region corresponding to ENS) into the CrPV genome between
317 the 1A and 2B coding sequences flanked by duplicate copies of the 1A cleavage site (Fig. 5a,
318 Fig. S8). The recombinant DcDV sequence was inserted into the CrPV genome such that ENS-
319 derived primary piRNAs mapping antisense to DcDV transcripts would map to the negative
320 strand of the recombinant CrPV-DcDV genome. Thus, in both cases, ENS-derived primary
321 piRNAs are complementary to the viral coding sequence and in analogy to the mechanisms of
322 ping-pong amplification in the context of TEs, should be theoretically capable of directing

323 cleavage of viral mRNAs. This recombinant virus is designated CrPV-DcDV. While the 57 nt
324 inserted region is relatively small in the context of the ~9 kb CrPV genome, piRNA target sites
325 corresponding to single piRNAs are known to be sufficient for induction of ping-pong
326 amplification and a single piRNA produced from a PCLV-derived EVE was proposed to mediate
327 a piRNA-based antiviral response in Aag2 cells (16,42–44). Additional analysis of the sRNA
328 mapping data from DcDV-uninfected CRF-CA *D. citri* shown in Figure 3a indicates that this 57
329 nt region gives rise to an average of 171.7 27-32 nt sRNAs made up of an average of 30.7 unique
330 sequences in the three sRNA libraries analyzed (data not shown).
331
332 We found that the virions produced following transfection of S2 cells with *in vitro* transcribed
333 CrPV-DcDV RNA were indistinguishable from those produced following transfection with wild-
334 type CrPV RNA (Fig. 5b & c) and RT-PCR of RNA purified from CrPV-DcDV virions indicated
335 that the recombinant sequence was retained (Fig. 5d). Finally, we found that infection of S2 cells
336 with either wild-type CrPV or CrPV-DcDV virions resulted in the cytopathic effects
337 characteristic of CrPV infection (Fig. 5e & f).
338
339 To determine whether ENS-derived piRNAs mediate a response to CrPV-DcDV in *D. citri*, we
340 inoculated CRF-CA *D. citri* with 1000 tissue culture infectious dose 50% ($TCID_{50}$) units of wild-
341 type CrPV or CrPV-DcDV per insect by intrathoracic injection. We observed a significant
342 difference in viral RNA levels for wild-type CrPV and CrPV-DcDV three days post injection
343 (Fig. 6a). By five days post injection, CrPV-DcDV RNA levels remained lower than those of
344 wild-type CrPV, but the difference was not statistically significant (Fig. 6a). RT-PCR results
345 indicated the recombinant DcDV sequence was retained throughout the course of infection with

346 CrPV-DcDV (Fig. S9). To determine if CrPV-DcDV was targeted by piRNAs, we sequenced
347 sRNAs from insects collected five days post infection. During infection with either virus, we
348 observed an abundance of 21 nt sRNAs of both polarities and these 21 nt sRNAs mapped to the
349 entire sequence of both viral genomes, indicating the presence of an siRNA-based response (Fig.
350 6b & c, Fig. S10 a & b). The recombinant DcDV sequence within the CrPV-DcDV genome was
351 a target of this siRNA-based response, as we observed abundant 21 nt sRNAs derived from this
352 portion of the recombinant virus genome in *D. citri* infected with CrPV-DcDV (Fig. 6d). When
353 sRNAs from *D. citri* infected with wild-type CrPV were mapped to the same DcDV-derived
354 sequence, a peak within the piRNA-size range was observed due to the production of piRNAs
355 from ENS, but no 21 nt peak was seen (Fig. 6e)
356
357 To evaluate whether CrPV-DcDV was targeted by ping-pong-dependent piRNAs, we analyzed
358 27-32 nt sRNAs separately depending on whether they mapped to the recombinant DcDV
359 sequence within the CrPV-DcDV genome or to the rest of the CrPV genome. We detected ENS-
360 derived antisense piRNAs mapping to the recombinant DcDV sequence in *D. citri* infected with
361 either wild-type CrPV or CrPV-DcDV (Fig. 6d-f), however, there was no evidence for the
362 production of ping-pong-dependent secondary piRNAs from this region during infection with
363 CrPV-DcDV (ping-pong Z-score = 0.28±0.18)(Fig. 6g & h). Ping-pong signatures were also not
364 observed for the non-recombinant portion of the CrPV-DcDV genome or for wild-type CrPV
365 (Fig. S10 c & d). These results indicate that CrPV-DcDV is not targeted by piRNAs during
366 infection initiated by intrathoracic injection in *D. citri* despite the presence of ENS-derived
367 piRNAs identical to the recombinant DcDV sequence.
368

369 Because the expression of ENS-derived piRNAs is highest in the gut (Fig. 3d) we wanted to
370 examine whether a piRNA-based response to CrPV-DcDV could be detected during infection
371 initiated by oral acquisition. Thus, we orally inoculated *D. citri* insects from CRF-CA with wild-
372 type CrPV or CrPV-DcDV by allowing the insects to feed for 96 hours on an artificial diet
373 solution containing 10^9 $TCID_{50}$ units/mL of wild-type CrPV or CrPV-DcDV. Following the 96
374 hour feeding period, the insects were transferred to *Citrus macrophylla* plants and viral RNA
375 levels were evaluated every three days by RT-qPCR. Viral RNA levels in the insects were nearly
376 identical for wild-type CrPV and CrPV-DcDV immediately following their removal from the
377 virus-containing artificial diet and average viral RNA levels increased in the days following
378 transfer of the insects to plants, although there was a substantial amount of variation between
379 biological replicates (Fig. 7a). As with infections initiated by intrathracic injection, RT-PCR
380 results indicated the recombinant DcDV sequence was retained throughout the course of oral
381 infection with CrPV-DcDV (Fig. S9b). These results suggest that while wild-type CrPV and
382 CrPV-DcDV are both infectious in *D. citri* following oral acquisition, individual insects
383 displayed a variety of infection outcomes. Similar results have previously been reported for
384 orally acquired infections with other RNA viruses in insects (45). We sequenced sRNAs from
385 insects collected nine days after transfer of the insects from the virus-containing artificial diet to
386 plants. We analyzed this data as described above for infections initiated by injection and found
387 that while both wild-type CrPV and CrPV-DcDV were targeted by siRNAs, neither virus was
388 targeted by ping-pong-dependent vpiRNAs during oral infection (ping-pong Z-score for 27-32 nt
389 sRNAs mapping to the recombinant DcDV sequence during CrPV-DcDV infection = 1.04 ±
390 0.67)(Fig. 7b-h). Together, our results indicate that despite the presence of endogenous primary
391 piRNAs complementary to a portion of the recombinant viral genome, CrPV-DcDV is not a

392 target of the piRNA pathway in *D. citri* following infection initiated either orally or by
393 intrathoracic injection.
394
395
396 **Discussion**
397 Primary vpiRNAs were first reported for American nodavirus, Drosophila C virus, Drosophila
398 tetravirus, Nora virus, Drosophila X virus, and Drosophila birnavirus in a *D. melanogaster*
399 ovarian somatic sheet (OSS) cell line (46). However, these conclusions were based only the size
400 of the sRNAs and nucleotide biases for all virus-specific sRNAs pooled into a single analysis. A
401 subsequent study using whole flies found no evidence for the production of primary or secondary
402 vpiRNAs during infection with Drosophila C virus, Drosophila X virus, Sindbis virus, Nora
403 virus, Drosophila A virus, Drosophila melanogaster sigma virus, invertebrate iridescent virus 6,
404 or Flock house virus (14). To date, ping-pong dependent vpiRNAs have only been found in a
405 small number of mosquito species and cells lines that express an expanded group of Piwi-family
406 Argonaute proteins.
407
408 Aedes albopictus densovirus 1 (AalDV-1) was recently shown to be a target of both siRNAs and
409 ping-pong-dependent vpiRNAs during persistent infection in *Ae. aegypti*-derived Aag2 cells,
410 representing the first report of vpiRNAs targeting a DNA virus and the first report of siRNAs
411 targeting a ssDNA virus in insects (47). Densoviruses replicate exclusively in the nucleus (48)
412 and interestingly, analysis of nuclear and cytoplasmic sRNA fractions of AalDV-1-infected Aag2
413 cells revealed that while AalDV-1-derived primary piRNAs are found in both the nucleus and
414 cytoplasm, ping-pong-dependent piRNAs targeting AalDV-1 are found only in the cytoplasm
415 (47). Ago3 and Piwi5 are the sole Piwi family proteins required for the production of vpiRNAs

416 during infection of Aag2 cells with Sindbis virus (9). As these proteins are expressed only in the
417 cytoplasm, the observation that AalDV-1-derived primary piRNAs are present in the nucleus
418 during infection of Aag2 cells suggests that a different pathway may generate primary vpiRNAs
419 from viral RNA in the nucleus (47). Such a pathway would be distinct from the cytoplasmic
420 Ago3/Piwi5 pathway that is responsible for production of vpiRNAs from Sindbis virus and
421 might rely on a piRNA biogenesis factor expressed in the nucleus, such as zucchini endonuclease
422 (47).
423
424 How viruses are marked as substrates for piRNA biogenesis remains unclear. In Aag2 cells, viral
425 and TE RNAs are processed into piRNAs by distinct sets of Piwi-family Argonaute proteins, but
426 it is unknown how viral RNA is recognized by these proteins (9). Moreover, as discussed above,
427 the presence of AalDV-1-derived primary piRNAs in the nucleus of Aag2 cells suggests that a
428 different pathway for the production of primary vpiRNAs may operate in the nucleus (47).
429 Several previous reports have speculated that primary piRNAs derived from EVEs may facilitate
430 the targeting of cognate viruses in a manner analogous to the targeting of TEs by the canonical
431 ping-pong cycle (15–17). Theoretically, such a targeting mechanism could facilitate the
432 production of vpiRNAs in species that do not express the expanded group of Piwi-family
433 Argonaute proteins expressed by some mosquito species and mosquito-derived cell lines.
434
435 The *D. citri* genome contains a DcDV-derived EVE (denoted ENS) with 86% nucleotide identity
436 to the corresponding portion of the DcDV genome and here we found that ENS serves as a
437 source for DcDV-specific primary piRNAs in geographically distinct *D. citri* populations.
438 However, we found that ENS is not present in all *D. citri* populations and that *D. citri* insects

439 lacking ENS do not produce endogenous DcDV-specific piRNAs. While more comprehensive
440 analyses are needed, comparing our results with the known geographic distribution of *D. citri*
441 lineages suggests that ENS may be present in lineage B *D. citri* and absent in lineage A *D. citri.*
442 We previously established a colony of *D. citri* insects harboring DcDV as a persistent infection
443 (CRF-TW)(34) and here we found that insects from this colony do not possess ENS. Sequencing
444 of sRNAs from *D. citri* insects from CRF-TW revealed the production of DcDV-derived ping-
445 pong-dependent vpiRNAs. Similar results were obtained by sequencing sRNAs from DcDV-
446 infected CRF-Uru *D. citri*, another *D. citri* population which does produce any endogenous
447 DcDV-specific piRNAs. These were surprising results, as the *D. citri* repertoire of Piwi-family
448 Argonaute proteins is limited to homologs of those expressed in *D. melanogaster,* which have so
449 far not been associated with the production of vpiRNAs (29,49). The production of vpiRNAs in
450 *D. citri* seems to display some virus specificity as vpiRNAs were not seen during infection with
451 Diaphorina citri reovirus, Diaphorina citri picrona-like virus, Diaphorina citri bunyavirus,
452 Diaphorina citri flavi-like virus, or CrPV. Notably, these viruses are all RNA viruses that
453 replicate in the cytoplasm, but DcDV is a DNA virus that replicates in the nucleus. While the
454 production of ping-pong-dependent DcDV-derived vpiRNAs is noteworthy, we cannot determine
455 whether this process plays an antiviral role based on the present data.
456
457 Densoviruses are known to replicate exclusively in the nucleus (48). Given that vpiRNAs are not
458 produced during infection of *D. citri* with positive strand RNA viruses, a negative strand RNA
459 virus, or a dsRNA virus, future analysis should determine whether DcDV RNA is processed into
460 primary vpiRNAs in the nucleus as was suggested for AalDV-1 (47). Interestingly, abundant
461 virus-derived sRNAs within the piRNA size range are also observed during infection of *Myzus*

462 *persicae* with Myzus persicae densovirus and during infection of *Culex pipiens molestus* with
463 Mosquito densovirus, however, these sRNAs were not analyzed for the presence of piRNA
464 signatures (50,51).
465
466 In addition to ping-pong dependent vpiRNAs, our results show that DcDV is also targeted by 21
467 nt siRNAs. RNA interference mediated by siRNAs is the primary antiviral defense mechanism
468 against RNA viruses in insects and requires cleavage of dsRNA substrates by the RNase III
469 enzyme dicer (52). RNA interference mediated by siRNAs is also known to target dsDNA
470 viruses and a ssDNA virus was recently shown to be targeted by siRNAs in Aag2 cells (47,53–
471 56). Previous reports have suggested that overlapping viral transcripts represent the dsRNA
472 substrate that becomes processed into siRNAs during infection with DNA viruses (47,53–55).
473 Indeed, we previously found that transcriptional readthrough during transcription of the
474 ambisense DcDV genome leads to the production of nearly genome length complementary
475 transcripts (34). These transcripts may anneal to form the dsRNA required for production of
476 siRNAs and may constitute the sense and antisense precursors required for the ping-pong cycle.
477
478 Although our results indicate that EVE-derived piRNAs are not required for the production of
479 ping-pong-dependent DcDV-derived vpiRNAs, we cannot exclude the possibility that EVE-
480 derived piRNAs could serve as an additional pool of piRNAs that could also contribute to
481 priming of the ping-pong cycle. Thus, to investigate whether EVE-derived piRNAs can prime
482 ping-pong amplification during infection with a virus sharing complementary sequence in *D.*
483 *citri*, we constructed CrPV-DcDV, a recombinant CrPV harboring 57 nt derived from the DcDV
484 genome and corresponding to ENS. Despite the presence of endogenous primary piRNAs

485 derived from ENS perfectly mapping to the recombinant region of CrPV-DcDV, we did not
486 observe induction of the ping-pong cycle during infection with this virus initiated either by oral
487 acquisition or intrathoracic injection of virions. The lack of ping-pong cycle activation during
488 infection with CrPV-DcDV is unlikely to be due to an absence of ping-pong activity in the
489 tissues infected by CrPV-DcDV, as we detected abundant TE-derived ping-pong-dependent
490 piRNAs in dissected *D. citri* guts, heads, hemolymph, ovaries, and testis. These results indicate
491 that the presence of EVE-derived primary piRNAs sharing perfect nucleotide identity with an
492 exogenous virus is not in itself sufficient to mark that virus as a target for ping-pong
493 amplification in *D. citri*. We note that our approach has some limitations. Host-responses to virus
494 infection are shaped by coevolution and there is a possibility that CrPV-DcDV was not targeted
495 by ping-pong-derived piRNAs due to differences in the infection cycles between DcDV (a
496 naturally infecting DNA virus) and CrPV (a non-naturally infecting RNA virus). For example,
497 these may include potential differences in the spatial or physical accessibility of viral RNA to
498 piRNA biogenesis factors. Indeed, our results suggest that RNA viruses are not targeted by
499 piRNAs in *D. citri*. Thus, it is possible that even if EVE-derived piRNAs could prime ping-pong
500 amplification during infection with a cognate DNA virus, cognate RNA viruses may not be
501 susceptible to such targeting by the piRNA pathway. Future research aiming to uncover the
502 mechanisms of vpiRNA production during infection with DNA viruses such as DcDV and
503 AalDV-1 will help to resolve these questions.
504
505 We previously reported that while DcDV persistently infects CRF-TW *D. citri,* CRF-CA *D. citri*
506 are not susceptible to DcDV infection by oral acquisition or intrathoracic injection (34). We
507 report here that CRF-Uru *D. citri* can be persistently infected with DcDV by either of these

508 routes of infection. As discussed above, CRF-TW and CRF-Uru *D. citri* are likely to be of
509 lineage A, while CRF-CA *D. citri* are likely to be of lineage B. At present, no genotypic or
510 phenotypic differences between the two lineages have been described except for nucleotide
511 variation within the mitochondrial cytochrome oxidase subunit I gene (30–32). Genetic
512 background is known to contribute to susceptibility to virus infection within different
513 populations of the same species (57). In the case of Densoviruses, a single arginine residue at
514 position 188 within a mucin-like glycoprotein expressed in the midgut epithelium of *Bombyx*
515 *mori* strains susceptible to infection with Bombyx mori densovirus (BmDV) was substituted by
516 other amino acids in resistant strains (58). Further analysis showed that this mucin-like
517 glycoprotein was the cellular receptor for BmDV in the midgut epithelium and that the arginine
518 residue at position 188 was required for BmDV binding to this protein (58). EVEs have been
519 suggested to play a role in susceptibility to virus infection through a variety of potential
520 mechanisms (16,59–61). Our results suggest that ENS is present in lineage B *D. citri,* but absent
521 in lineage A *D. citri* and that the presence of ENS correlates with resistance to DcDV infection in
522 the populations tested. However, other genetic differences between the two lineages are likely to
523 exist and we cannot assess whether ENS may be involved with resistance to DcDV infection
524 based on the present data. Nevertheless, our data highlight both a genetic and phenotypic
525 difference between the two *D. citri* lineages. Other such differences between the lineages and
526 how they may contribute to susceptibility to DcDV infections should be the subject of future
527 investigations.
528
529
530 **Materials and methods**

531 *Maintenance of* D. citri *insects*

532 *D. citri* insects were reared on *C. macrophylla* plants in mesh cages (BugDorm, Taichung,
533 Taiwan) at 25 ± 2 °C under a 14:10 hour (light:dark) photoperiod and 60-70% relative humidity
534 at the University of California Davis CRF (62). *D. citri* insects from Uruguay and Taiwan were
535 imported under USDA APHIS-PPQ permit P526P-17-02906 by shipping adults and nymphs on
536 *C. macrophylla* or *Murraya paniculata* cuttings, respectively.

537

538

539 *sRNA sequencing and analysis*

540 For total insect sRNA sequencing of CRF-CA, CRF-TW, and CRF-Uru *D. citri*, total RNA was
541 extracted from groups of 50 adult *D. citri* insects using TRIzol reagent (Invitrogen, Carlsbad,
542 California) according to the manufacturer's instructions, but omitting the 75% ethanol wash. For
543 CRF-CA *D. citri* infected with wild-type CrPV or CrPV-DcDV by oral acquisition or injection
544 and for the progeny CRF-Uru *D. citri* infected with DcDV by injection, sRNAs were extracted
545 from groups of 25 adult *D. citri* insects using TRIzol reagent according to the manufacturer's
546 instructions, but omitting the 75% ethanol wash. For organ specific sRNA sequencing multiple
547 dissected organs were combined to be processed as one sample: 200 for gut, head, or hemolymph
548 and 100 for ovary or testis. RNA extraction was done from pooled organ samples with the
549 Direct-zol RNA Miniprep kit (Zymo Research, Irvine, California) following the manufacturer's
550 instructions. Three pooled samples of each organ were used. For all sRNA sequencing, total
551 RNA was sent to Beijing Genomics Institute for library prep with the TruSeq small RNA sample
552 preparation kit (Illumina, San Diego, California) and sequencing by 50 bp single end sequencing
553 with the BGISEQ-500 platform. For all sRNA reads, adaptor sequences were removed with Trim

554 Galore version 0.4.4 (63) and the fastxtoolkit was used to remove reads containing bases with
555 quality score <20 (64). The remaining reads were mapped to viral genomes, insect genomes, or
556 TEs using BowTie version 1.2.1.1 (65) using the default settings with the following exceptions: -
557 n 1 -l 20. When only perfectly mapped reads were considered (specifically indicated in the text),
558 the –v 0 option was used instead of the –n 1 –l 20 options. Sequence logos were produced using
559 WebLogo 3 (66). Ping-pong Z-scores were calculated with signature.py (67). All sRNA
560 sequence data generated for this study was deposited to the NCBI SRA database (BioProject
561 accession no. PRJNA629895).
562
563
564 *Analysis of EVEs*
565 DcDV-derived EVEs were identified in *D. citri* genomic scaffold 2850 by BLASTx using as
566 queries the deduced amino acid sequences of DcDV structural and non-structural proteins
567 (GenBank accession no.'s YP_009256210, YP_009256211, YP_009256212, and
568 YP_009256213). DcDV-derived EVEs were then inspected by aligning the DcDV genome
569 (GenBank accession no. NC_030296) to the nucleotide sequence of *D. citri* genomic scaffold
570 2850 using ClustalW (68). Deduced amino acid and nucleotide identities shared between ENS
571 and DcDV and between EITR and DcDV were calculated as p-distance with complete deletion
572 of gaps from ClustalW alignments using MEGA 7 (69).
573
574
575 *Identification of TEs*

576 We identified TEs present within the *D. citri* genome using RepeatMasker version 4.0.6 (70)
577 with the Metazoa library. In addition, to identify TEs lacking homology to previously annotated
578 TEs, we used RepeatModeler version 1.0.8 (71) to produce a *de novo* hidden Markov model for
579 TEs within the *D. citri* genome which was subsequently used as input for a second analysis using
580 RepeatMasker. All TE identification was performed using TEAnnotator.py as previously
581 described to produce a single strand-specific .fasta file containing the sequences of all TEs >100
582 nt identified in the *D. citri* genome (35).
583
584
585 *Nucleic acid extraction, reverse transcription, PCR, exonuclease digestion, and Sanger*
586 *sequencing*
587 Unless otherwise specified, DNA was extracted from groups of 25 homogenized *D. citri* insects
588 by phenol/chloroform extraction followed by ethanol precipitation. For PCR using exonuclease
589 treated DNA, 1 µg CRF-CA *D. citri* genomic DNA, an intact plasmid containing the ENS
590 amplicon, or the same plasmid digested overnight with HindIII-HF and SbfI-HF (New England
591 Biolabs, Ipswich, Massachusetts) were digested overnight with 10 units of Plasmid-Safe ATP-
592 Dependent DNAse (Lucigen, Middleton, Wisconsin) according to the manufacturer's
593 instructions. For analysis of ENS transcription, RNA was extracted from groups of 25
594 homogenized CRF-CA *D. citri* using TRIzol reagent according to the manufacturer's
595 instructions. RNA was treated twice with the Qiagen RNAse-free DNAse set (Qiagen, Hilden,
596 Germany) to remove DNA. cDNA was prepared from 50 ng RNA with SuperScript IV reverse
597 transcriptase (Invitrogen, Carlsbad, California) using specific primers (see the legend for Fig. 1)
598 according to the manufacturer’s instructions. To assess retention of the insert in CrPV-DcDV,

599 RNA was extracted from CrPV or CrPV-DcDV virions using TRIzol LS (Invitrogen, Carlsbad,
600 California) according to the manufacturer's instructions. cDNA was prepared from 50 ng virion
601 RNA using the Applied Biosystems high capacity reverse transcription kit (Applied Biosystems,
602 Foster City, California) using random primers according to the manufacturer's instructions and
603 cDNA was diluted 1:10 prior to PCR. Primer sequences are given in supplementary Table 1 and
604 their use is described in the appropriate figure legends. All PCR reactions were performed with
605 CloneAmp HiFi PCR premix (Takara Bio, Mountain View, California) using 25 ng of DNA, 1 µl
606 of cDNA (for determination of ENS transcription), or 3 µl diluted cDNA (for determination of
607 CrPV-DcDV insertion retention). Detailed PCR protocols are available upon request. PCR
608 products were analyzed by 0.8% or 2% agarose gel electrophoresis and visualized under UV
609 after staining with SYBR safe DNA gel stain (Invitrogen, Carlsbad, California). PCR products
610 were purified with the Zymoclean Gel DNA Recovery Kit (Zymo Research, Irvine, California)
611 and sequenced by Quintarabio using the Sanger method.
612
613
614 *Southern blotting*
615 5 µg undigested CRF-CA *D citri* DNA or 5 µg CRF-CA *D. citri* DNA digested overnight with
616 PstI-HF and HindIII-HF (New England Biolabs, Ibswich, Massachusetts) was electrophoresed in
617 a 0.8% agarose/0.5x TAE gel and the gel was prepared for transfer by incubation in 0.25 M HCl
618 for 30 minutes, then 0.5 M NaCl, 0.5 M NaOH for 30 minutes, and then 1.5 M NaCl, 0.5 M Tris-
619 HCl pH 7 for 30 minutes. DNA was then transferred to an Amersham Hybond Nx membrane
620 (GE Life Sciences, Boston, Massachusetts) for 24 hours in 20X SSC using the capillary method.

621 DNA was cross-linked to the membrane by exposure to 120,000 µjoles of UV light using a UV
622 Stratalinker 2400 (Stratagene, San Diego, California).
623
624 A PCR product corresponding to ENS was prepared by PCR with primers 27 and 3 using CRF-
625 CA *D. citri* DNA as a template. This PCR product was then used a template to prepare a
626 radioactive RNA probe by *in vitro* transcription using the MAXIscript T7 Transcription Kit
627 (Invitrogen, Carlsbad, California) with 32P-UTP according to the manufacturer's instructions.
628
629 The membrane with cross-linked DNA was prehybridized by incubation in Ambion ULTRAhyb
630 Ultrasensitive hybridization buffer (Invitrogen, Carlsbad, California) for 2 hours at 42 °C in a
631 rotary incubation oven. Following prehybridization, 2 x 10^6 CPM/mL radioactive probe was
632 added and hybridization proceeded for 16 hours at 42 °C in a rotary incubation oven. The
633 membrane was then washed at 42 °C for 15 minutes each with 2X SSC/0.1% SDS, 0.2X
634 SSC/0.1% SDS, and 0.1X SSC/0.1% SDS.
635
636
637 *DcDV infections and DcDV qPCR*
638 DcDV virions were partially purified from 0.5 g of CRF-TW *D. citri* as previously described
639 (34). The number of DcDV genome copies in the virion preparation was determined by qPCR
640 with primers 29 and 30 (see table S1) as described previously (34). For infections by
641 intrathoracic injection, the virion preparations were diluted to 8.2 x 10^5 genome copies/µl in 100
642 mM Tris-HCl, pH 7.5. Adult CRF-Uru *D. citri* were anesthetized on ice for approximately 15
643 minutes and intrathoracicly injected with approximately 200 nl of the diluted virion preparation

644 by manual injection using a syringe fitted to a 34 gauge stainless steel needle (Hamilton, Reno,
645 Nevada). Following injection, insects were maintained on *C. macrophylla* plants. For infections
646 by oral acquisition, the virion preparations were diluted to 8.2 x 10^5 genome copies/µl in 15%
647 sucrose, 0.1% green food coloring, 0.4% yellow food coloring prepared in 100 mM Tris-HCl, pH
648 7.5. Groups of 30 adult CRF-Uru *D. citri* were fed on the virus-containing sucrose solution for
649 96 hours by membrane feeding as described previously (34). Following the feeding period,
650 insects were maintained on *C. macrophylla* plants. Day 0 is designated as the day insects were
651 transferred from the virus containing artificial diet to plants. For both types of infection, adult
652 insects (>1 day old) were used and neither age nor gender of the insects was determined prior to
653 infection.
654
655 For both types of infection, five pools of three insects were collected every two days and DNA
656 was purified from each pool by phenol/chloroform extraction followed by ethanol precipitation
657 as described previously (34). All insects had been collected or were removed from the plants by
658 17 days post infection. During the maintenance period on plants, the DcDV-injected and -fed
659 insects laid eggs on the plants. Following removal of the DcDV-injected or –fed insects, the
660 plants were maintained to allow development of the progeny. The progeny were removed on the
661 day of emergency to the adult stage and DNA was extracted from 10 individual progeny insects
662 from each experiment as described above. A pool of 25 progeny of the DcDV-injected *D. citri*
663 was collected at the same time for sRNA purification. The concentration of DcDV genome
664 copies in the DNA pools or in DNA extracted from individual progeny insects was assessed by
665 qPCR with primers 29 and 30 (see Fig. S1) using 25 ng DNA as described previously (34).
666 Technical triplicates were used for all qPCR reactions.

667

668

669 *Cloning of CrPV-DcDV*

670 Complementary lyophilized oligonucleotides containing the DcDV sequence to be inserted
671 flanked upstream by 15 nt corresponding to the 3' end of the CrPV 1A nucleotide sequence and
672 downstream by 15 nt corresponding to the 5' end of the CrPV 2B nucleotide sequence were
673 suspended to a concentration of 100 µM in 100 mM potassium acetate, 300 µM HEPES, pH 7.5
674 (oligo sequences: 5'-
675 TCTAATCCTGGTCCTGCAGACCGTTCACCTTCTCCAGGACCTTCTACTGCATATCGCT
676 ATTGTAGCGAGGAAGTGCAATCGCGCCCC and 5' –
677 GGGGCGCGATTGCACTTCCTCGCTACAATAGCGATATGCAGTAGAAGGTCCTGGAG
678 AAGGTGAACGGTCTGCAGGACCAGGATTAGA). To anneal these oligonucleotides, the
679 oligonucleotides were mixed in equimolar ratios, incubated at 94 °C for 3 minutes, and allowed
680 to cool slowly to room temperature to form the duplex oligo. pCrPV-3 (a gift from Shou-Wei
681 Ding) (72) was linerized by inverse PCR with primers 13 and 14 and the duplex oligo was
682 ligated to the linearized plasmid in a 2:1 insert:vector molar ratio using NEBuilder Hifi
683 Assembly Master Mix (New England Biolabs, Ipswich, Massachusetts) according to the
684 manufacturer's instructions. The resulting plasmid (designated pCrPV-1A-DcDV) was
685 transformed into chemically competent *E. coli* DH5α and transformed cells were grown on luria
686 bertani (LB) agar plates containing 100 µg/mL ampicillin at 28 °C for 16 hours. Insert presence
687 was verified by colony PCR with primers 15 and 17 and by Sanger sequencing of colony PCR
688 products. Colonies containing the desired plasmid were used to inoculate 5 mL LB broth
689 containing 100 µg/mL ampicillin and the cultures were incubated at 28 °C for 16 hours with 220

690 rpm shaking. Plasmids were purified from overnight cultures with the QIAprep Spin Miniprep
691 Kit (Qiagen, Hilden, Germany) according to the manufacturer's instructions.
692
693 To duplicate the 1A cleavage site on the 3' end of the recombinant DcDV sequence, pCrPV-1A-
694 DcDV was linearized by inverse PCR with primers 17 and 18 and the linearized plasmid was
695 circularized by blunt end ligation with T4 DNA ligase (New England Biolabs, Ipswich,
696 Massachusetts) according to the manufacturer's instructions to create pCrPV-1A-DcDV-1A. The
697 ligation product was transformed into chemically competent *E. coli* DH5α and plasmids were
698 purified as described.
699
700
701 *Transfection and infection of S2 Cells and virion purification*
702 pCrPV-3 and pCrPV-1A-DcDV-1A were linearized by digestion with BamHI-HF (New England
703 Biolabs, Ipswich, Massachusetts). Wild-type and CrPV-DcDV RNA was prepared by *in vitro*
704 transcription of 1 µg linearized plasmid using the mMESSAGE mMACHINE T7 transcription
705 kit (Invitrogen, Carlsbad, California) according to the manufacturer's instructions. 24 hours prior
706 to transfection, 5 x 10^6 S2 cells were seeded in 2 mL Schneider's Drosophila media (Thermo
707 Fisher, Waltham, Massachusetts) supplemented with 10% heat-inactivated fetal bovine serum in
708 9.6 cm^2 wells of a tissue culture plate and incubated at 26 °C. The following day, cells were
709 transfected with wild-type CrPV or CrPV-DcDV RNA using the TransMessenger transfection
710 reagent (Qiagen, Hilden, Germany) according to the manufacturer's instructions and the
711 transfected cells were incubated at 26 °C. After 72 hours, 1 mL of transfected cells was
712 transferred to a 50 mL tissue culture flask containing 3 x 10^6 S2 cells/mL that had been passed

713 24 hours prior in 6 mL Schneider's Drosophila media supplemented with 10% heat-inactivated
714 fetal bovine serum. After incubation at 26 °C for 96 hours, virions were purified from the
715 infected S2 cells by centrifugation at 8,000 RPM for 10 minutes at 4 °C using a Beckman GSA
716 rotor (Beckman Coulter, Brea, California). The supernatant was then collected and centrifuged at
717 8,000 RPM for 30 minutes at 4 °C using a Beckman GSA rotor. The supernatant was collected
718 and centrifuged through a 15% sucrose cushion (prepared in 10 mM Tris-HCl, pH 7.5) at 45,000
719 RPM for 45 minutes at 11 °C in a Beckman 70.1 Ti rotor (Beckman Coulter, Brea, California).
720 The pellet was resuspended in 10 mM Tris-HCl, pH 7.5 and then filtered through a 0.22 µm
721 filter.
722
723 The titer of purified CrPV-DcDV or CrPV virions was measured by end-point dilution. Briefly, 4
724 x 10^5 S2 cells were seeded in 500 µL Schneider's Drosophila media supplemented with 10%
725 heat-inactivated fetal bovine serum in each well of 24 well plates. Cells were incubated for 24
726 hours at 26°C. After 24 hours cells were infected with tenfold serial dilutions of purified virions
727 in 100 µL volumes. Dilutions over the range of 10^{-5} to 10^{-10} were used and six individual wells
728 were used for each dilution. After 72 hours, cells were examined for the presence cytopathic
729 effects and the titer of the undiluted virus stock was calculated from these results using the Reed
730 and Muench method.
731
732 For infection of S2 cells using purified virions, 5 x 10^6 S2 cells were seeded in 2 mL Schneider's
733 Drosophila media supplemented with 10% heat-inactivated fetal bovine serum in 9.6 cm^2 wells
734 of a tissue culture plate and incubated at 26 °C. After 24 hours, 100 $TCID_{50}$ units of wild-type

735 CrPV or CrPV-DcDV virions suspended in 100 µL Schneider's Drosophila media were added to
736 the wells.
737
738
739 *Microscopy*
740 Wild-type CrPV or CrPV-DcDV virions (see above) were further purified by centrifugation
741 through a 1.2 g/cm^3 to 1.6 g/cm^3 cesium chloride density gradient at 50,000 RPM for 4 hours at
742 11 °C in a Beckman SW 65 Ti rotor (Beckman Coulter, Brea, California). Visible "virus bands"
743 in the gradients were collected using a Hamilton syringe and diluted 1:10 in 10 mM Tris-HCl,
744 pH 7.5. Diluted virions were then centrifuged at 75,000 RPM for 30 minutes at 11 °C in a
745 Beckman TLA 120 rotor (Beckman Coulter, Brea, California). The pellet was resuspended in 10
746 mM Tris-HCl, pH 7.5 and negatively stained with uranyl formate. Negatively stained virion
747 samples were observed by transmission electron microscopy using a JEOL 1230 electron
748 microscope (JEOL, Tokyo, Japan) operating at 100 kV. Mock-infected S2 cells and S2 cells
749 infected with wild-type CrPV or CrPV-DcDV were observed by bright-field microscopy using a
750 Leica DM5000B microscope (Leica, Wetzlar, Germany).
751
752
753 *CrPV infections in* D. citri
754 Adult CRF-CA *D. citri* were infected with purified CrPV or CrPV-DcDV virions by
755 intrathoracic injection or membrane feeding exactly as described above for DcDV infections. For
756 injections, purified virions were diluted to 5000 $TCID_{50}$ units/µl and insects were injected with
757 approximately 200 nl each. Seven pools of three insects each were collected on days 0, 3, 6, and

758 9 for RNA extraction. Three additional pools of 25 insects each were collected on day 9 for
759 sRNA extraction. For membrane feeding, purified virions were diluted to 10^9 $TCID_{50}$ units/µl.
760 Five pools of three insects each were collected on days 0, 3, and 5 for RNA extraction. Three
761 additional pools of 25 insects each were collected on day 5 for sRNA extraction.
762 To determine viral RNA levels, RNA was extracted from the pools of three insects using TRIzol
763 reagent according to the manufacturer's instructions. RNA pellets were resuspended in 25 µl
764 water and cDNA was prepared from 1 µl RNA (approximately 200-400 ng RNA) with the high
765 capacity cDNA reverse transcription kit using random primers according to the manufacturer's
766 instructions and cDNA was diluted 1:10. Wild-type CrPV and CrPV-DcDV RNA levels were
767 determined using 4.5 µL diluted cDNA for qPCR reactions with the SsoAdvanced Universal
768 SYBR Green Supermix (BioRad, Hercules, California) in 10 µL reactions. Primers 19 and 20
769 were used for CrPV RNA and primers 21 and 22 were used for *D. citri* actin. All primers were
770 used at a final concentration of 0.25 nM. The qPCR reaction conditions consisted of an initial
771 denaturation at 98 °C for 2 min followed by 40 cycles at 95 °C for 10 s and 60 °C for 20 s.
772 CrPV RNA levels were normalized based on the expression of *D. citri* actin using the $2^{-\Delta\Delta Ct}$
773 method (73). Technical triplicates were used for al qPCR reactions. Diluted cDNA from each
774 day was pooled to assess retention of the insert in CrPV-DcDV as described above.
775
776
777 **Acknowledgements**
778 We thank colleagues who provided us *D. citri* samples: W.O. Dawson, H. Wuriyanghan, H.-H
779 Yeh, Y. Cen, A. M. Khan, M. A. Machado, T. da Silva, D. M. Galdeano, D. Jenkins, C. Higashi,
780 A. Chow, D. Morgan, K. Pelz-Stelinski, K. Godfrey, B. Baker, G. Simmons, M. Keremane, and

781 J. Buenahora. We thank S.W.-Ding for providing us with pCrPV-3. We also thank M-C. Saleh
782 for critical reading of the manuscript. The U.S. Department of Agriculture provided funding to
783 Bryce W. Falk under grant numbers 13-002NU-781 and 2015-70016-23011. This material is
784 based upon work supported by the National Science Foundation Graduate Research Fellowship
785 Program under Grant No. 1650042.

786

787

788 **Competing interests**

789 The authors declare that they have no competing interests.

790

791

792 **References**

793 1. Czech B, Hannon GJ. One loop to rule them all: the ping-pong cycle and piRNA-guided
794 silencing. Trends Biochem Sci. 2016;41(4):324–37.

795 2. Dietrich I, Jansen S, Fall G, Lorenzen S, Rudolf M, Huber K, et al. RNA interference
796 restricts Rift Valley Fever virus in multiple insect systems. MSphere. 2017;2(3):e00090-
797 17.

798 3. Varjak M, Maringer K, Watson M, Sreenu VB, Fredericks AC, Pondeville E, et al. Aedes
799 aegypti Piwi4 is a noncanonical PIWI protein involved in antiviral responses. MSphere.
800 2017;2(3):e00144-17.

801 4. Dietrich I, Shi X, McFarlane M, Watson M, Blomström A-L, Skelton JK, et al. The
802 antiviral RNAi response in vector and non-vector cells against orthobunyaviruses. PLoS

803 Negl Trop Dis. 2017;11(1):e0005272.

804 5. Schnettler E, Donald CL, Human S, Watson M, Siu RWC, McFarlane M, et al.
805 Knockdown of piRNA pathway proteins results in enhanced Semliki Forest virus
806 production in mosquito cells. J Gen Virol. 2013;94:1680-89.

807 6. Brennecke J, Aravin AA, Stark A, Dus M, Kellis M, Sachidanandam R, et al. Discrete
808 small RNA-generating loci as master regulators of transposon activity in Drosophila. Cell.
809 2007;128(6):1089–103.

810 7. Vodovar N, Bronkhorst AW, Van Cleef KWR, Miesen P, Blanc H, Van Rij RP, et al.
811 Arbovirus-derived piRNAs exhibit a ping-pong signature in mosquito cells. PLoS One.
812 2012;7(1):e30861.

813 8. Leger P, Lara E, Jagla B, Sismeiro O, Mansuroglu Z, Coppée JY, et al. Dicer-2-and Piwi-
814 mediated RNA interference in Rift Valley fever virus-infected mosquito cells. J Virol.
815 2013;87(3):1631–48.

816 9. Miesen P, Girardi E, van Rij RP. Distinct sets of PIWI proteins produce arbovirus and
817 transposon-derived piRNAs in Aedes aegypti mosquito cells. Nucleic Acids Res.
818 2015;43(13):6545–56.

819 10. Miesen P, Ivens A, Buck AH, van Rij RP. Small RNA profiling in dengue virus 2-infected
820 Aedes mosquito cells reveals viral piRNAs and novel host miRNAs. PLoS Negl Trop Dis.
821 2016;10(2):e0004452.

822 11. Morazzani EM, Wiley MR, Murreddu MG, Adelman ZN, Myles KM. Production of virus-
823 derived ping-pong-dependent piRNA-like small RNAs in the mosquito soma. PLoS

824 Pathog. 2012;8(1):e1002470.

825 12. Goic B, Stapleford KA, Frangeul L, Doucet AJ, Gausson V, Blanc H, et al. Virus-derived
826 DNA drives mosquito vector tolerance to arboviral infection. Nat Commun.
827 2016;7:12410.

828 13. Campbell CL, Black WC, Hess AM, Foy BD. Comparative genomics of small RNA
829 regulatory pathway components in vector mosquitoes. BMC Genomics. 2008;9(1):425.

830 14. Petit M, Mongelli V, Frangeul L, Blanc H, Jiggins F, Saleh M-C. piRNA pathway is not
831 required for antiviral defense in Drosophila melanogaster. Proc Natl Acad Sci.
832 2016;113(29):E4218–27.

833 15. ter Horst AM, Nigg JC, Dekker FM, Falk BW. Endogenous Viral Elements Are
834 Widespread in Arthropod Genomes and Commonly Give Rise to PIWI-Interacting RNAs.
835 J Virol. 2019;93(6):e02124-18.

836 16. Whitfield ZJ, Dolan PT, Kunitomi M, Tassetto M, Seetin MG, Oh S, et al. The diversity,
837 structure, and function of heritable adaptive immunity sequences in the Aedes aegypti
838 genome. Curr Biol. 2017;27(22):3511–9.

839 17. Palatini U, Miesen P, Carballar-Lejarazu R, Ometto L, Rizzo E, Tu Z, et al. Comparative
840 genomics shows that viral integrations are abundant and express piRNAs in the arboviral
841 vectors Aedes aegypti and Aedes albopictus. BMC Genomics. 2017;18(1):512.

842 18. Katzourakis A, Gifford RJ. Endogenous viral elements in animal genomes. PLoS Genet.
843 2010;6(11):e1001191.

844 19. François S, Filloux D, Roumagnac P, Bigot D, Gayral P, Martin DP, et al. Discovery of

845 parvovirus-related sequences in an unexpected broad range of animals. Sci Rep.
846 2016;6:30880.

847 20. Suzuki Y, Frangeul L, Dickson LB, Blanc H, Verdier Y, Vinh J, et al. Uncovering the
848 repertoire of endogenous flaviviral elements in Aedes mosquito genomes. J Virol.
849 2017;91(15):e00571-17.

850 21. Tassetto M, Kunitomi M, Whitfield ZJ, Dolan PT, Sánchez-Vargas I, Garcia-Knight M, et
851 al. Control of RNA viruses in mosquito cells through the acquisition of vDNA and
852 endogenous viral elements. Elife. 2019;8:e41244.

853 22. Grafton-Cardwell EE, Stelinski LL, Stansly PA. Biology and management of Asian citrus
854 psyllid, vector of the huanglongbing pathogens. Annu Rev Entomol. 2013;58:413–32.

855 23. Singerman A, Rogers ME. The economic challenges of dealing with citrus greening: The
856 case of Florida. J Integr Pest Manag. 2020;11(1):3.

857 24. Tiwari S, Mann RS, Rogers ME, Stelinski LL. Insecticide resistance in field populations
858 of Asian citrus psyllid in Florida. Pest Manag Sci. 2011;67(10):1258–68.

859 25. Juan-Blasco M, Qureshi JA, Urbaneja A, Stansly PA. Predatory mite, Amblyseius swirskii
860 (Acari: Phytoseiidae), for biological control of Asian citrus psyllid, Diaphorina citri
861 (Hemiptera: Psyllidae). Florida Entomol. 2012;95(3):543–51.

862 26. Étienne J, Quilici S, Marival D, Franck A. Biological control of Diaphorina citri
863 (Hemiptera: Psyllidae) in Guadeloupe by imported Tamarixia radiata (hymenoptera:
864 Eulophidae). Fruits. 2001;56(5):307–15.

865 27. Hajeri S, Killiny N, El-Mohtar C, Dawson WO, Gowda S. Citrus tristeza virus-based

866 RNAi in citrus plants induces gene silencing in Diaphorina citri, a phloem-sap sucking
867 insect vector of citrus greening disease (Huanglongbing). J Biotechnol. 2014;176:42–9.

868 28. Nouri S, Salem N, Nigg JC, Falk BW. Diverse array of new viral sequences identified in
869 worldwide populations of the Asian citrus psyllid (Diaphorina citri) using viral
870 metagenomics. J Virol. 2016;90(5):2434–45.

871 29. Saha S, Hosmani PS, Villalobos-Ayala K, Miller S, Shippy T, Flores M, et al. Improved
872 annotation of the insect vector of citrus greening disease: biocuration by a diverse
873 genomics community. Database. 2017;2017:bax032.

874 30. Luo Y, Agnarsson I. Global mt DNA genetic structure and hypothesized invasion history
875 of a major pest of citrus, Diaphorina citri (Hemiptera: Liviidae). Ecol Evol.
876 2018;8(1):257–65.

877 31. De León JH, Sétamou M, Gastaminza GA, Buenahora J, Cáceres S, Yamamoto PT, et al.
878 Two separate introductions of Asian citrus psyllid populations found in the American
879 continents. Ann Entomol Soc Am. 2011;104(6):1392–8.

880 32. Boykin LM, De Barro P, Hall DG, Hunter WB, McKenzie CL, Powell CA, et al.
881 Overview of worldwide diversity of Diaphorina citri Kuwayama mitochondrial
882 cytochrome oxidase 1 haplotypes: two Old World lineages and a New World invasion.
883 Bull Entomol Res. 2012;102(5):573–82.

884 33. Goic B, Vodovar N, Mondotte JA, Monot C, Frangeul L, Blanc H, et al. RNA-mediated
885 interference and reverse transcription control the persistence of RNA viruses in the insect
886 model Drosophila. Nat Immunol. 2013;14(4):396.

887 34. Nigg JC, Falk BW. Diaphorina citri densovirus is a persistently infecting virus with a
888 hybrid genome organization and unique transcription strategy. J Gen Virol. 2020;101:226-
889 239.

890 35. Lewis SH, Quarles KA, Yang Y, Tanguy M, Frézal L, Smith SA, et al. Pan-arthropod
891 analysis reveals somatic piRNAs as an ancestral defence against transposable elements.
892 Nat Ecol Evol. 2018;2(1):174.

893 36. Matsumura EE, Nerva L, Nigg JC, Falk BW, Nouri S. Complete Genome Sequence of the
894 Largest Known Flavi-Like Virus, Diaphorina citri flavi-like virus, a Novel Virus of the
895 Asian Citrus Psyllid, Diaphorina citri. Genome Announc. 2016;4(5):e00946-16.

896 37. Marutani-Hert M, Hunter WB, Katsar CS, Sinisterra XH, Hall DG, Powell CA. Reovirus-
897 like sequences isolated from adult Asian citrus psyllid,(Hemiptera: Psyllidae: Diaphorina
898 citri). Florida Entomol. 2009;92(2):314–21.

899 38. Chen Q, Godfrey K, Liu J, Mao Q, Kuo Y-W, Falk BW. A nonstructural protein
900 responsible for viral spread of a novel insect reovirus provides a safe channel for
901 biparental virus transmission to progeny. J Virol. 2019;93(15):e00702-19.

902 39. Reinganum C, O'Loughlin G., Hogan TW. A nonoccluded virus of the field crickets
903 Teleogryllus océaniens and T.commodus (Orthoptera: Gryllidae). J Invertebr Pathol.
904 1970;16:216–20.

905 40. Nayak A, Berry B, Tassetto M, Kunitomi M, Acevedo A, Deng C, et al. Cricket paralysis
906 virus antagonizes Argonaute 2 to modulate antiviral defense in Drosophila. Nat Struct Mol
907 Biol. 2010;17(5):547.

908 41. Costa A, Jan E, Sarnow P, Schneider D. The Imd pathway is involved in antiviral immune
909 responses in Drosophila. PLoS One. 2009;4(10):e7436.

910 42. Barckmann B, Pierson S, Dufourt J, Papin C, Armenise C, Port F, et al. Aubergine iCLIP
911 reveals piRNA-dependent decay of mRNAs involved in germ cell development in the
912 early embryo. Cell Rep. 2015;12(7):1205–16.

913 43. Bagijn MP, Goldstein LD, Sapetschnig A, Weick E-M, Bouasker S, Lehrbach NJ, et al.
914 Function, targets, and evolution of Caenorhabditis elegans piRNAs. Science (80-).
915 2012;337(6094):574–8.

916 44. Mohn F, Handler D, Brennecke J. piRNA-guided slicing specifies transcripts for
917 Zucchini-dependent, phased piRNA biogenesis. Science. 2015;348(6236):812–7.

918 45. Mondotte JA, Gausson V, Frangeul L, Blanc H, Lambrechts L, Saleh M-C. Immune
919 priming and clearance of orally acquired RNA viruses in Drosophila. Nat Microbiol.
920 2018;3(12):1394.

921 46. Wu Q, Luo Y, Lu R, Lau N, Lai EC, Li W-X, et al. Virus discovery by deep sequencing
922 and assembly of virus-derived small silencing RNAs. Proc Natl Acad Sci.
923 2010;107(4):1606–11.

924 47. Parry R, Bishop C, De Hayr L, Asgari S. Density-dependent enhanced replication of a
925 densovirus in Wolbachia-infected Aedes cells is associated with production of piRNAs
926 and higher virus-derived siRNAs. Virology. 2019;528:89–100.

927 48. Tijssen P, Bando H, Li Y, Jousset F, Zadori Z, Fediere G, et al. Evolution of densoviruses.
928 Parvoviruses. 2005;5:55–60.

929 49. Taning CNT, Andrade EC, Hunter WB, Christiaens O, Smagghe G. Asian citrus psyllid
930 RNAi pathway–RNAi evidence. Sci Rep. 2016;6:38082.

931 50. Pinheiro P V, Wilson JR, Xu Y, Zheng Y, Rebelo AR, Fattah-Hosseini S, et al. Plant
932 Viruses Transmitted in Two Different Modes Produce Differing Effects on Small RNA-
933 Mediated Processes in Their Aphid Vector. Phytobiomes J. 2019;3(1):71–81.

934 51. Ma M, Huang Y, Gong Z, Zhuang L, Li C, Yang H, et al. Discovery of DNA viruses in
935 wild-caught mosquitoes using small RNA high throughput sequencing. PLoS One.
936 2011;6(9):e24758.

937 52. Bronkhorst AW, van Rij RP. The long and short of antiviral defense: small RNA-based
938 immunity in insects. Curr Opin Virol. 2014;7:19–28.

939 53. Bronkhorst AW, van Cleef KWR, Vodovar N, İnce İA, Blanc H, Vlak JM, et al. The DNA
940 virus Invertebrate iridescent virus 6 is a target of the Drosophila RNAi machinery. Proc
941 Natl Acad Sci. 2012;109(51):E3604–13.

942 54. Jayachandran B, Hussain M, Asgari S. RNA interference as a cellular defense mechanism
943 against the DNA virus baculovirus. J Virol. 2012;86(24):13729–34.

944 55. Karamipour N, Fathipour Y, Talebi AA, Asgari S, Mehrabadi M. Small interfering RNA
945 pathway contributes to antiviral immunity in Spodoptera frugiperda (Sf9) cells following
946 Autographa californica multiple nucleopolyhedrovirus infection. Insect Biochem Mol
947 Biol. 2018;101:24–31.

948 56. Kemp C, Mueller S, Goto A, Barbier V, Paro S, Bonnay F, et al. Broad RNA
949 interference–mediated antiviral immunity and virus-specific inducible responses in

950 Drosophila. J Immunol. 2013;190(2):650–8.

951 57. Palmer WH, Varghese FS, Van Rij RP. Natural variation in resistance to virus infection in
952 dipteran insects. Viruses. 2018;10(3):118.

953 58. Ito K, Kidokoro K, Katsuma S, Sezutsu H, Uchino K, Kobayashi I, et al. A single amino
954 acid substitution in the Bombyx-specific mucin-like membrane protein causes resistance
955 to Bombyx mori densovirus. Sci Rep. 2018;8(1):7430.

956 59. Klenerman P, Hengartner H, Zinkernagel RM. A non-retroviral RNA virus persists in
957 DNA form. Nature. 1997;390(6657):298.

958 60. Fujino K, Horie M, Honda T, Merriman DK, Tomonaga K. Inhibition of Borna disease
959 virus replication by an endogenous bornavirus-like element in the ground squirrel genome.
960 Proc Natl Acad Sci. 2014;111(36):13175–80.

961 61. Maori E, Tanne E, Sela I. Reciprocal sequence exchange between non-retro viruses and
962 hosts leading to the appearance of new host phenotypes. Virology. 2007;362(2):342–9.

963 62. Galdeano DM, Breton MC, Lopes JRS, Falk BW, Machado MA. Oral delivery of double-
964 stranded RNAs induces mortality in nymphs and adults of the Asian citrus psyllid,
965 Diaphorina citri. PLoS One. 2017;12(3):e0171847.

966 63. Krueger F. Trim galore. A wrapper tool around Cutadapt FastQC to consistently apply
967 Qual Adapt trimming to FastQ files. 2015;

968 64. Gordon A, Hannon GJ. Fastx-toolkit. FASTQ/A short-reads preprocessing tools
969 (unpublished) http://hannonlab cshl edu/fastx_toolkit. 2010;5.

970 65. Langmead B. Aligning short sequencing reads with Bowtie. Curr Protoc Bioinforma.
971 2010;32(1):11–7.

972 66. Crooks GE, Hon G, Chandonia JM, Brenner SE. WebLogo: A sequence logo generator,
973 Genome Research. WebLogo a Seq logo Gener Genome Res. 2004;14(6).

974 67. Antoniewski C. Computing siRNA and piRNA overlap signatures. In: Animal Endo-
975 SiRNAs. Springer; 2014. p. 135–46.

976 68. Larkin MA, Blackshields G, Brown NP, Chenna R, McGettigan PA, McWilliam H, et al.
977 Clustal W and Clustal X version 2.0. bioinformatics. 2007;23(21):2947–8.

978 69. Kumar S, Stecher G, Tamura K. MEGA7: molecular evolutionary genetics analysis
979 version 7.0 for bigger datasets. Mol Biol Evol. 2016;33(7):1870–4.

980 70. Smit A, Hubley R, Green P. RepeatMasker Open-4.0 [Internet]. 2013-2015. Available
981 from: http://www.repeatmasker.org

982 71. Smit A, Hubley R. RepeatModeler Open-1.0 [Internet]. 2008. Available from:
983 http://www.repeatmasker.org/RepeatModeler/

984 72. Kerr CH, Wang QS, Keatings K, Khong A, Allan D, Yip CK, et al. The 5′ untranslated
985 region of a novel infectious molecular clone of the dicistrovirus cricket paralysis virus
986 modulates infection. J Virol. 2015;89(11):5919–34.

987 73. Schmittgen TD, Livak KJ. Analyzing real-time PCR data by the comparative C T method.
988 Nat Protoc. 2008;3(6):1101.

989

990 **Fig. 1**
991

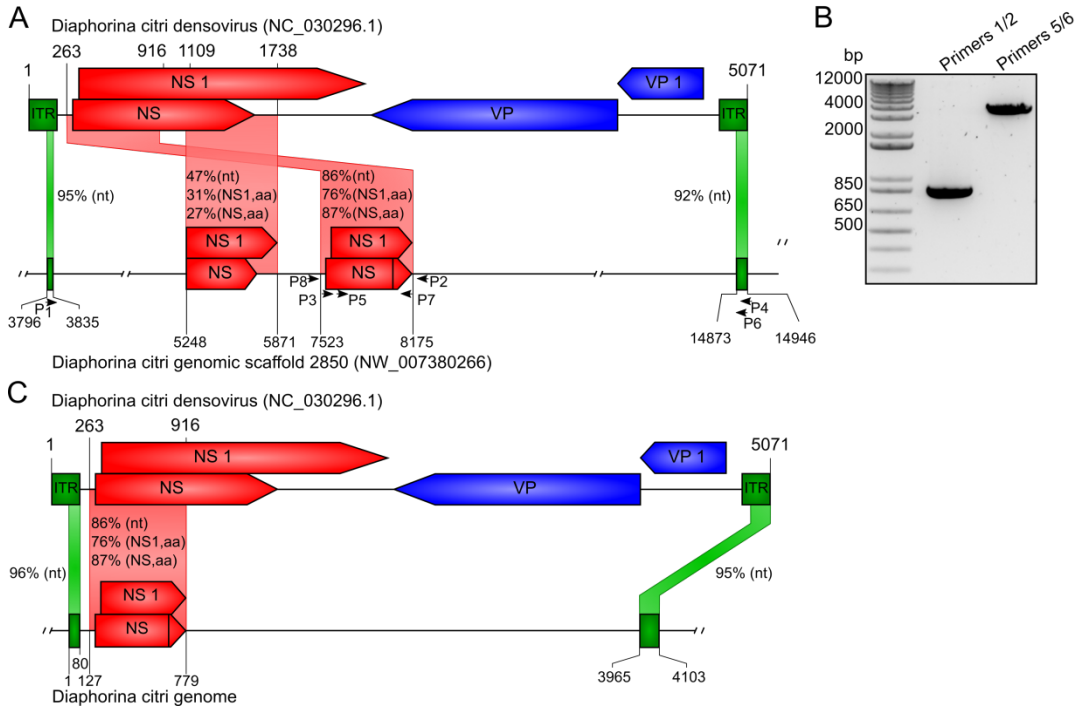

992
993

994 **Fig. 1.** A DcDV-like EVE is present in the *D. citri* genome. (A) Organization of DcDV-derived
995 EVEs identified in *D. citri* genomic scaffold 2850 by BLASTx followed by manual sequence
996 alignment. The DcDV genome organization is shown on top with the corresponding region of
997 scaffold 2850 on the bottom. Numbers above and below the sequence depictions represent
998 nucleotide positions. Vertical lines inside shaded boxes represent stop codons. The percent
999 nucleotide or deduced amino acid (aa) identity between EVEs and corresponding viral genomic
1000 regions/proteins is given. Annealing positions of PCR primers are shown with arrows. (B)
1001 Confirmation of EVE presence by PCR using primers shown in panel A. The product produced
1002 with primers 5/6 was produced by nested PCR using as template a 1:1000 dilution of a PCR
1003 product produced with primers 3/4. (C) The correct organization of the region of the *D. citri*
1004 genome containing ENS and EITR, as confirmed by sequencing of the PCR products shown in
1005 panel B.
1006
1007
1008
1009
1010
1011
1012
1013
1014
1015
1016
1017

1018 **Fig. 2**
1019

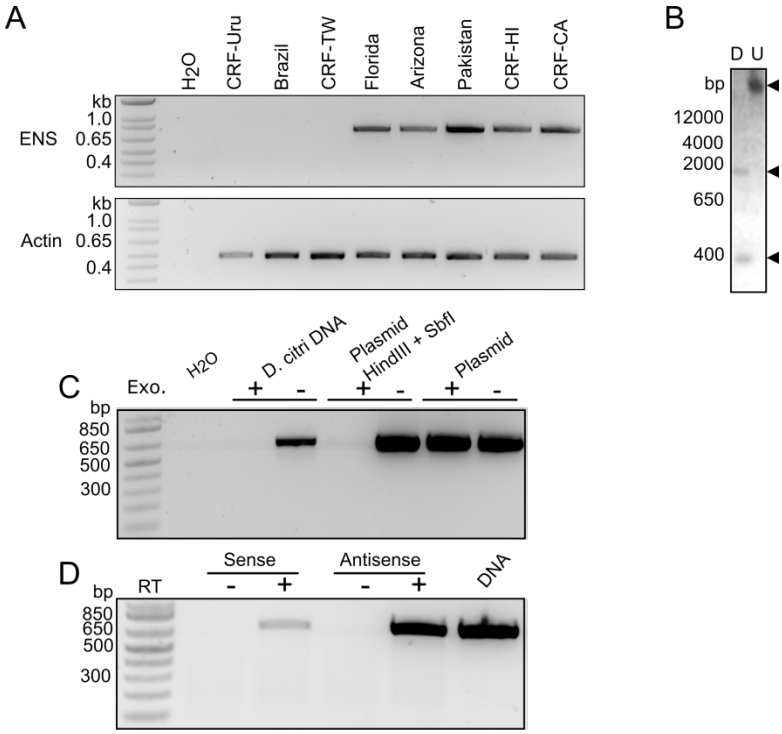

1020
1021
1022 **Fig 2.** ENS is a transcribed EVE that is unevenly distributed among distinct *D. citri* populations.
1023 (A) Upper: PCR products produced using primers flanking ENS (primers 2 and 8). Lower: PCR
1024 products produced using primers specific to *D. citri* actin (primers 9 and 10). (B) Southern blot
1025 of *D. citri* genomic DNA using an RNA probe based on the sequence of ENS; U = undigested, D
1026 = digested with PstI and HindIII. Upper arrow denotes ENS in undigested genomic DNA. Lower
1027 arrows denote cleavage products. (C) PCR products produced using primers 3 and 7 and the
1028 indicated DNA samples. "Plasmid" is a plasmid containing the full ENS sequence and "Plasmid
1029 HindIII + SbfI" is the same plasmid digested with HindIII and SbfI. DNA was left intact or
1030 digested with an exonuclease (Exo.) prior to PCR. (D) Primers 3 or 7 were used to generate
1031 cDNA from antisense or sense transcripts, respectively. cDNAs were used as templates for PCR
1032 using primers 3 and 7. DNA or cDNA prepared without reverse transcriptase (RT) served as
1033 controls.
1034
1035
1036
1037
1038
1039
1040
1041
1042
1043
1044
1045

1046 **Fig. 3**
1047

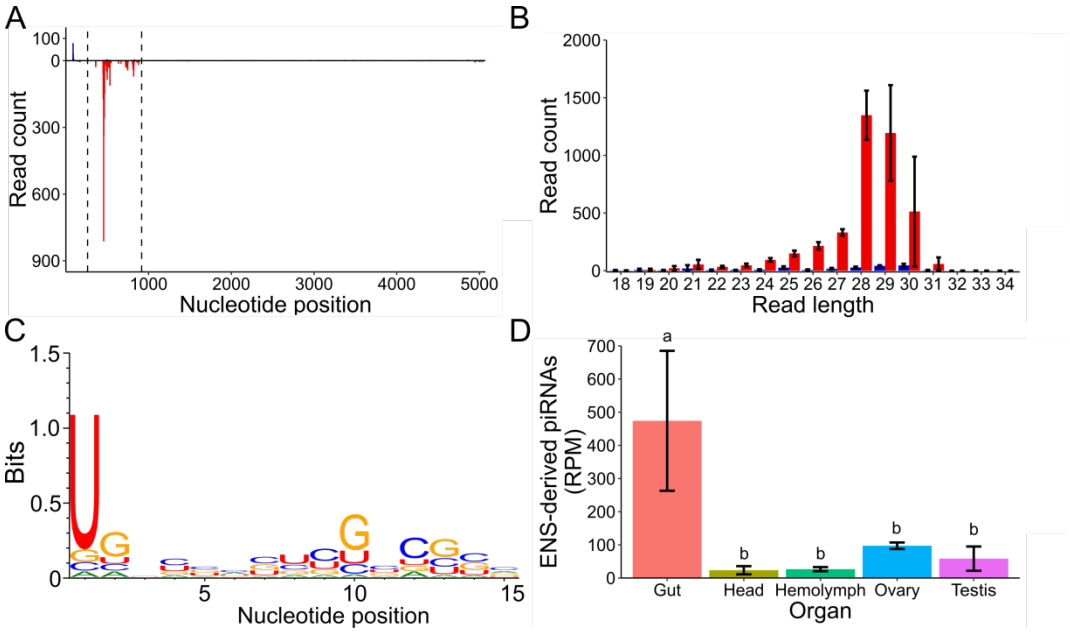

1048
1049

1050 **Fig. 3.** DcDV-specific piRNAs are produced from ENS in *D. citri* from CRF-CA. (A) Positions
1051 of all sRNAs from CRF-CA *D. citri* mapped to the DcDV genome. Dashed lines indicate the
1052 region of the DcDV genome corresponding to ENS. sRNAs are shown as mapped to the genomic
1053 strand containing the coding sequence for the NS proteins. Red = antisense sRNAs, blue = sense
1054 sRNAs. Reads counts are an average of three independent libraries. (B) Length distribution of
1055 sRNAs shown in (A). Red = antisense, blue = sense. Read counts are an average of three
1056 independent libraries. Error bars indicate standard deviation. (C) Sequence logo of sRNAs shown
1057 in (A). Data represents three pooled libraries. (D) Abundance of 27-32 nt sRNAs from CRF-CA
1058 *D. citri* mapping to ENS in the indicated tissue types. Read counts for each library were
1059 normalized using the read counts per million mapped reads method (RPM)(59). Normalized read
1060 counts represent the average of three independent libraries. Error bars indicate standard
1061 deviation. Average RPM values for each tissue were compared by one-way ANOVA and
1062 Turkey's honestly significant difference post-hoc test. Significance is indicated by lowercase
1063 letters and tissues sharing a letter do not have significantly different RPM values ($p < 0.05$).
1064
1065
1066
1067
1068
1069
1070
1071
1072
1073
1074
1075
1076

1077 **Fig. 4**
1078

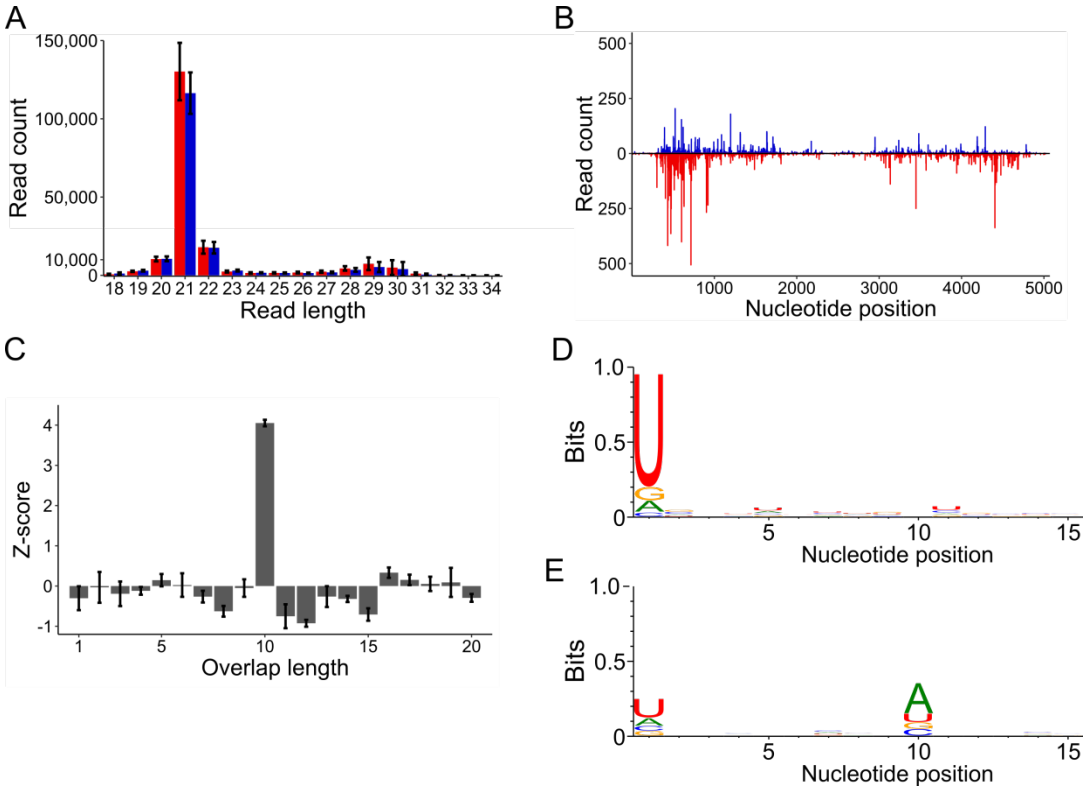

1079
1080
1081 **Fig. 4.** DcDV is targeted by ping-pong-dependent vpiRNAs in DcDV-infected *D. citri* insects
1082 from CRF-TW. (A) Length distribution of sRNAs mapping to the DcDV genome in DcDV-
1083 infected *D. citri* insects from CRF-TW. To account for the bidirectional transcription strategy of
1084 DcDV, sRNA mapping polarity was assigned from mapping location based on the start and stop
1085 positions of the canonical DcDV transcripts. Red = antisense sRNAs, blue = sense sRNAs. Read
1086 counts are an average of three independent libraries. Error bars indicate standard deviation. (B)
1087 Positions of 27-32 nt sRNAs shown in (A). Red = antisense sRNAs, blue = sense sRNAs. Read
1088 counts are an average of three independent libraries. (C) Z-scores for the indicated overlap
1089 distances between the 5' ends of complementary 27-32 nt sRNAs shown in (A). Z-scores are an
1090 average of three independent libraries. Error bars indicate standard deviation. (D & E) Sequence
1091 logos for the 27-32 nt sRNAs shown in (A). Sequence logos for antisense sRNAs (D) or sense
1092 sRNAs (E) are shown. Data represents three pooled libraries.
1093
1094
1095
1096
1097
1098
1099
1100
1101
1102

1103 **Fig. 5**
1104

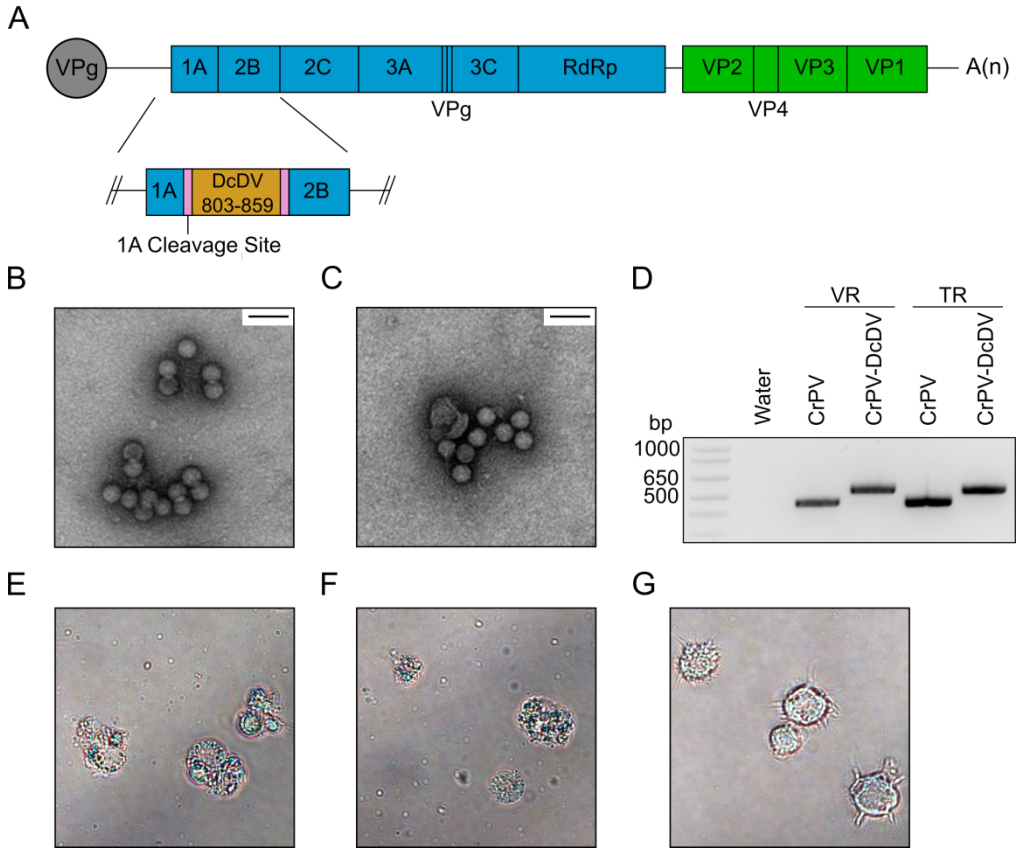

1105
1106

1107 **Fig. 5.** Construction of CrPV-DcDV, a recombinant CrPV mutant containing 57 nt of sequence
1108 from the DcDV genome. (A) Genome organization of CrPV DcDV. Blue rectangles represent
1109 the CrPV non-structural proteins. RdRp = RNA dependent RNA polymerase. VPg = viral protein
1110 genome-linked. Green boxes represent the CrPV structural proteins. The orange rectangle
1111 represents the recombinant DcDV sequence, which corresponds to nucleotides 803-859 from the
1112 DcDV genome. Pink rectangles represent the cleavage site at which the 1A protein is released
1113 from the polyprotein. (B & C) Electron micrographs of wild-type CrPV (B) or CrPV-DcDV (C)
1114 virions purified from S2 cells transfected with viral RNA. 50,000x magnification. Scale bar is 50
1115 nm. (D) RT-PCR products produced using primers flanking the site into which recombinant
1116 DcDV sequence was inserted in CrPV-DcDV (primers 11 and 12). RNA extracted from purified
1117 virions (VR) or *in vitro* transcribed viral RNA (TR) was used as a template. (E-G) Bright-field
1118 microscopy images of S2 cells infected with wild-type CrPV virions (E), CrPV-DcDV virions
1119 (F), or mock infected (G). Images were acquired 72 hours post-infection.
1120
1121
1122
1123
1124
1125
1126

1127 **Fig. 6**
1128

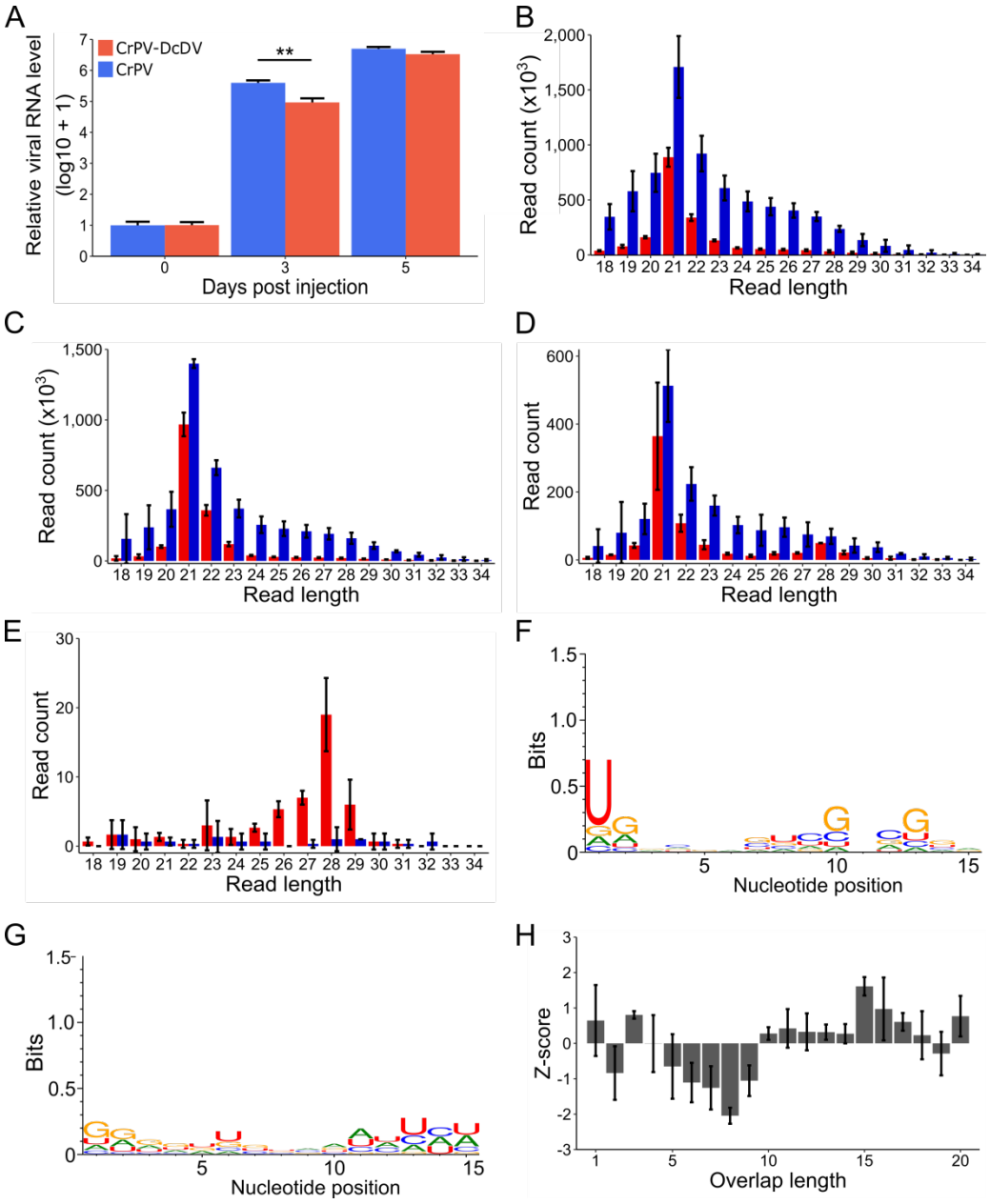

1129
1130

1131 **Fig. 6.** CrPV-DcDV is not targeted by piRNAs during infection initiated by intrathoracic
1132 injection of purified virions. (A) Relative viral RNA levels during infection with wild-type CrPV
1133 or CrPV-DcDV. Infection was initiated by intrathoracic injection of CRF-CA *D. citri* with 1000
1134 $TCID_{50}$ units of purified virions per insect. Viral RNA levels were assessed by RT-qPCR and
1135 normalized based on the expression of actin. The amount of viral RNA present on day 0 was set
1136 as 1 and log10 + 1 levels of viral RNA are shown relative to this value. Bars represent the
1137 average viral RNA level in five pools of three insects. Error bars indicate the standard error of
1138 the mean. ** = $p < 0.01$, two-tailed T-test. (B-F) analysis of sRNA sequencing data of sRNAs
1139 purified from CRF-CA *D. citri* infected with wild-type CrPV or CrPV-DcDV by intrathoracic

1140 injection as described for (A). sRNA was purified from pools of 25 *D. citri* collected 5 days post
1141 injection. (B) Length distribution of sRNAs from wild-type CrPV-infected *D. citri* mapped to the
1142 wild-type CrPV genome. Red = antisense, blue = sense. Read counts are an average of three
1143 independent libraries. Error bars indicate standard deviation. (C) Length distribution of sRNAs
1144 from CrPV-DcDV-infected *D. citri* mapped to the CrPV-DcDV genome. Red = antisense, blue =
1145 sense. Read counts are an average of three independent libraries. Error bars indicate standard
1146 deviation. (D) Length distribution of sRNAs from CrPV-DcDV-infected *D. citri* mapped to the
1147 recombinant DcDV sequence present within the CrPV-DcDV genome. Red = antisense, blue =
1148 sense. Read counts are an average of three independent libraries. Error bars indicate standard
1149 deviation. (E) Length distribution of sRNAs from wild-type CrPV-infected *D. citri* mapped to
1150 the recombinant DcDV sequence present within the CrPV-DcDV genome. Red = antisense, blue
1151 = sense. Read counts are an average of three independent libraries. Error bars indicate standard
1152 deviation. (F & G) Sequence logos for 27-32 nt sRNAs from CrPV-DcDV-infected *D. citri*
1153 mapped to the recombinant DcDV sequence present within the CrPV-DcDV genome. Sequence
1154 logos for antisense sRNAs (F) or sense sRNAs (G) are shown. Data represents three pooled
1155 libraries. (H) Probability of overlap between the 5' ends of complementary 27-32 nt sRNAs
1156 mapping to opposite strands of the recombinant DcDV sequence present within the CrPV-DcDV
1157 genome during infection with CrPV-DcDV. Probabilities are shown for the indicated overlap
1158 distances and represent the average of three independent libraries. Error bars indicate standard
1159 deviation. The average Z-score and the standard deviation of the Z-score for an overlap length of
1160 10 nt is shown
1161
1162
1163
1164
1165
1166
1167
1168
1169
1170
1171
1172
1173
1174
1175
1176
1177
1178
1179
1180
1181
1182
1183
1184
1185

1186 **Fig. 7**
1187

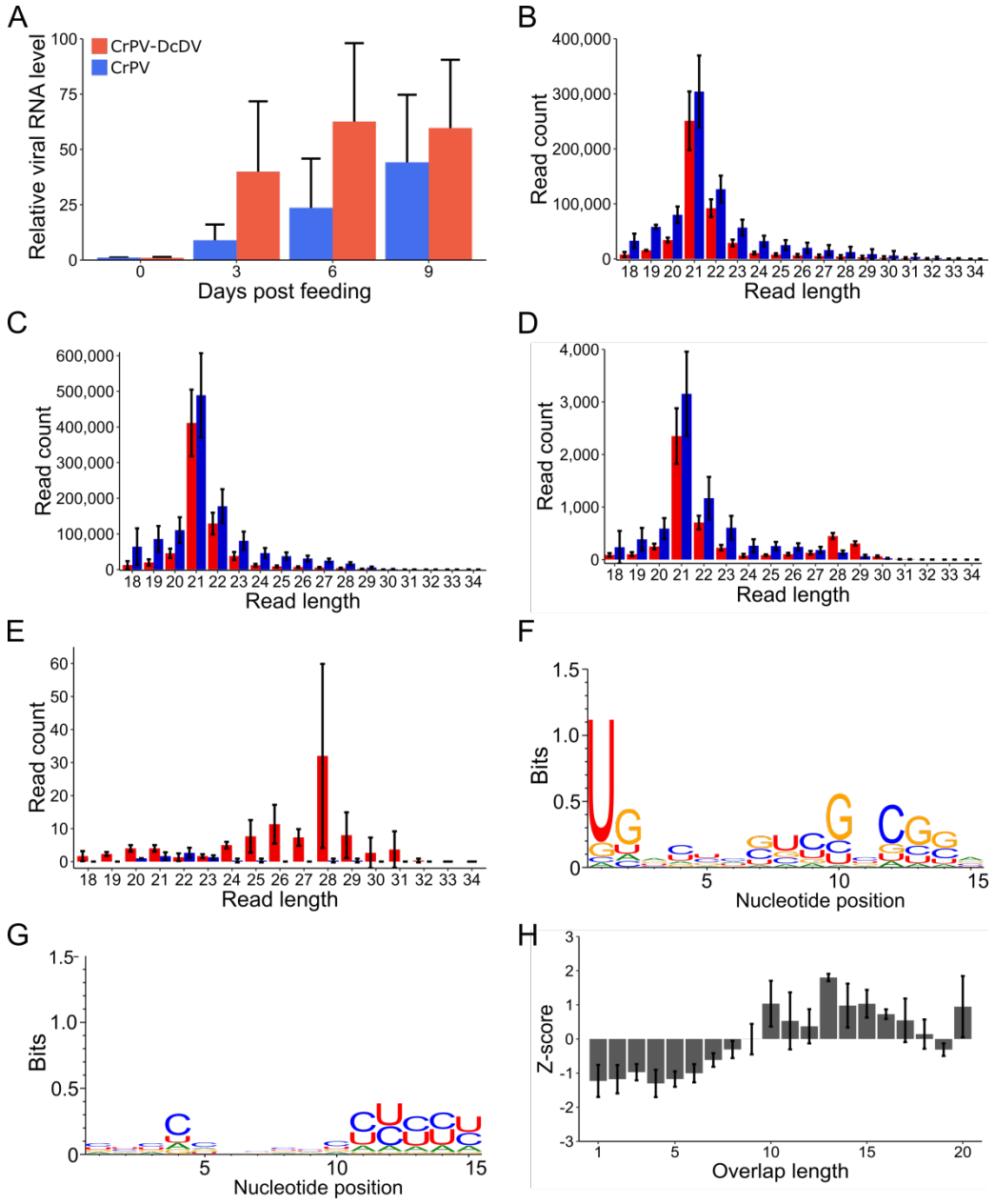

1188
1189

1190 **Fig. 7.** CrPV-DcDV is not targeted by piRNAs during infection initiated by oral acquisition of
1191 purified virions. (A) Relative viral RNA levels during infection with wild-type CrPV or CrPV-
1192 DcDV. Infection was initiated in CRF-CA *D. citri* by oral acquisition. Insects were allowed to
1193 feed for 96 hours on an artificial diet solution containing 10^9 $TCID_{50}$ units/mL of wild-type
1194 CrPV or CrPV-DcDV. Following the feeding period insects were moved to *C. macrophylla*
1195 plants (day 0 post feeding). Viral RNA levels were assessed by RT-qPCR and normalized based
1196 on the expression of actin. The amount of viral RNA present on day 0 was set as 1 and viral
1197 RNA levels are shown relative to this value. Bars represent the average viral RNA level in seven
1198 pools of three insects. Error bars indicate the standard error of the mean. (B-F) analysis of sRNA

1199 sequencing data of sRNAs purified from CRF-CA *D. citri* infected with wild-type CrPV or
1200 CrPV-DcDV by oral acquisition as described for (A). sRNA was purified from pools of 25 *D.*
1201 *citri* collected 9 days post feeding. (B) Length distribution of sRNAs from wild-type CrPV-
1202 infected *D. citri* mapped to the wild-type CrPV genome. Red = antisense, blue = sense. Read
1203 counts are an average of three independent libraries. Error bars indicate standard deviation. (C)
1204 Length distribution of sRNAs from CrPV-DcDV-infected *D. citri* mapped to the CrPV-DcDV
1205 genome. Red = antisense, blue = sense. Read counts are an average of three independent
1206 libraries. Error bars indicate standard deviation. (D) Length distribution of sRNAs from CrPV-
1207 DcDV-infected *D. citri* mapped to the recombinant DcDV sequence present within the CrPV-
1208 DcDV genome. Red = antisense, blue = sense. Read counts are an average of three independent
1209 libraries. Error bars indicate standard deviation. (E) Length distribution of sRNAs from wild-
1210 type CrPV-infected *D. citri* mapped to the recombinant DcDV sequence present within the
1211 CrPV-DcDV genome. Red = antisense, blue = sense. Read counts are an average of three
1212 independent libraries. Error bars indicate standard deviation. (F & G) Sequence logos for 27-32
1213 nt sRNAs from CrPV-DcDV-infected *D. citri* mapped to the recombinant DcDV sequence
1214 present within the CrPV-DcDV genome. Sequence logos for antisense sRNAs (F) or sense
1215 sRNAs (G) are shown. Data represents three pooled libraries. (H) Probability of overlap between
1216 the 5' ends of complementary 27-32 nt sRNAs mapping to opposite strands of the recombinant
1217 DcDV sequence present within the CrPV-DcDV genome during infection with CrPV-DcDV.
1218 Probabilities are shown for the indicated overlap distances and represent the average of three
1219 independent libraries. Error bars indicate standard deviation. The average Z-score and the
1220 standard deviation of the Z-score for an overlap length of 10 nt is shown.
1221
1222
1223
1224
1225
1226
1227
1228
1229
1230
1231
1232
1233
1234
1235

Fig. S1

```
CRF-CA   AAAGCGATAA GTTGTCGTAT AAATAGTGGT GTTGGTAGCA TTGTAACTTT AGTATGGACT GTTCA [ 65]
Florida  AAAGCGATAA GTTGTCGTAT AAATAGTGGT GTTGGTAGCA TTGTAACTTT AGTATGGACT GTTCA [ 65]
Pakistan AAAGCGATAA GTTGTCGTAT AAATAGTGGT GTTGGTAGCA TTGTAACTTT AGTATGGACT GTTCA [ 65]
Arizona  AAAGCGATAA GTTGTCGTAT AAATAGTGGT GTTGGTAGCA TTGTAACTTT AGTATGGACT GTTCA [ 65]
CRF-HI   AAAGCGATAA GTTGTCGTAT AAATAGTGGT GTTGGTAGCA TTGTAACTTT AGTATGGACT GTTCA [ 65]

CRF-CA   GCAGCGAGAA AATTTGAACG TCTTGATTGC GTGTGTTATT TTTGTCTTTT ACCAAAATTG CCAAC [130]
Florida  GCAGCGAGAA AATTTGAACG TCTTGATTGC GTGTGTTATT TTTGTCTTTT ACCAAAATTG CCAAC [130]
Pakistan GCAGCGAGAA AATTTGAACG TCTTGATTGC GTGTGTTATT TTTGTCTTTT ACCAAAATTG CCAAC [130]
Arizona  GCAGCGAGAA AATTTGAACG TCTTGATTGC GTGTGTTATT TTTGTCTTTT ACCAAAATTG CCAAC [130]
CRF-HI   GCAGCGAGAA AATTTGAACG TCTTGATTGC GTGTGTTATT TTTGTCTTTT ACCAAAATTG CCAAC [130]

CRF-CA   ACCAGTAGTG AATTTAGTTC CGACGAGGAT GAGTTCCGAC GAGGATTCGT GTCACTCGGT GATCG [195]
Florida  ACCAGTAGTG AATTTAGTTC CGACGAGGAT GAGTTCCGAC GAGGATTCGT GTCACTCGGT GATCG [195]
Pakistan ACCAGTAGTG AATTTAGTTC CGACGAGGAT GAGTTCCGAC GAGGATTCGT GTCACTCGGT GATCG [195]
Arizona  ACCAGTAGTG AATTTAGTTC CGACGAGGAT GAGTTCCAAC GAGGATTCGT GTCACTCGGT GATCG [195]
CRF-HI   ACCAGTAGTG AATTTAGTTC CGACGAGGAT GAGTTCCGAC GAGGATTCGT GTCACTCGGT GATCG [195]

CRF-CA   AGGAGGATCC TCTGAGTTCT GCTCCAGCGA GTCCGGCGAC GAGTCAACAT GGTCACAACT TAAGC [260]
Florida  AGGAGGATCC TCTGAGTTCT GCTCCAGCGA GTCCGGCGAC GAGTCAACAT GGTCACAACT TAAGC [260]
Pakistan AGGAGGATCC TCTGAGTTCT GCTCCAGCGA GTCCGGCGAC GAGTCAACAT GGTCACAACT TAAGC [260]
Arizona  AGGAGGATCC TCTGAGTTCT GCTCCAGCGA GTCCGGCGAC GAGTCAACAT GGTCACAACT TAAGC [260]
CRF-HI   AGGAGGATCC TCTGAGTTCT GCTCCAGCGA GTCCGGCGAC GAGTCAACAT GGTCACAACT TAAGC [260]

CRF-CA   GATTCCGAGG AGACGAACTG TACCGTCGTG TTGGCACAGA ATCCCCTGCC CGACACACAA GAAGT [325]
Florida  GATTCCGAGG AGACGAACTG TACCGTCGTG TTGGCACAGA ATCCCCTGCC CGACACACAA GAAGT [325]
Pakistan GATTCCGAGG AGACGAACTG TACCGTCGTG TTGGCACAGA ATCCCCTGCC CGACACACAA GAAGT [325]
Arizona  GATTCCGAGG AGACGAACTG TACCGTCGTG TTGGCACAGA ATCCCCTGCC CGACACACAA GAAGT [325]
CRF-HI   GATTCCGAGG AGACGAACTG TACCGTCGTG TTGGCACAGA ATCCCCTGCC CGACACACAA GAAGT [325]

CRF-CA   CGAATCGATG TTTCAAGAAG ACCGGAGCGC ATCAGTACAT TTCGCAGACG ATCCTCCGAC GGGAG [390]
Florida  CGAATCGATG TTTCAAGAAG ACCGGAGCGC ATCAGTACAT TTCGCAGACG ATCCTCCGAC GGGAG [390]
Pakistan CGAATCGATG TTTCAAGAAG ACCGGAGCGC ATCAGTACAT TTCGCAGACG ATCCTCCGAC GGGAG [390]
Arizona  CGAATCGATG TTTCAAGAAG ACCGGAGCGC ATCAGTACAT TTCGCAGACG ATCCTCCGAC GGGAG [390]
CRF-HI   CGAATCGATG TTTCAAGAAG ACCGGAGCGC ATCAGTACAT TTCGCAGACG ATCCTCCGAC GGGAG [390]

CRF-CA   CCCGGAAGAA GAAATCTATT CTGAAACGGG CGACGAAAAA GAAAACGACT CCCAAAGCGA ACACA [455]
Florida  CCCGGAAGAA GAAATCTATT CTGAAACGGG CGACGAAAAA GAAAACGACT CCCAAAGCGA ACACA [455]
Pakistan CCCGGAAGAA GAAATCTATT CTGAAACGGG CGACGAAAAA GAAAACGACT CCCAAAGCGA ACACA [455]
Arizona  CCCGGAAGAA GAAATCTATT CTGAAACGGG CGACGAAAAA GAAAACGACT CCCAAAGCGA ACACA [455]
CRF-HI   CCCGGAAGAA GAAATCTATT CTGAAACGGG CGACGAAAAA GAAAACGACT CCCAAAGCGA ACACA [455]

CRF-CA   GCGAAGAAGA TGCTCACTCT GACTCCTCAG CAACAGACAT CAGTGTGGGA ACGGCAAACC AACAA [520]
Florida  GCGAAGAAGA TGCTCACTCT GACTCCTCAG CAACAGACAT CAGTGTGGGA ACGGCAAACC AACAA [520]
Pakistan GCGAAGAAGA TGCTCACTCT GACTCCTCAG CAACAGACAT CAGTGTGGGA ACGGCAAACC AACAA [520]
Arizona  GCGAAGAAGA TGCTCACTCT GACTCCT-AG CAACAGACAT CAGTGTGGGA ACGGCAAACC AACAA [520]
CRF-HI   GCGAAGAAGA TGCTCACTCT GACTCCTCAG CAACAGACAT CAGTGTGGGA ACGGCAAACC AACAA [520]

CRF-CA   CTTTATGGCA TTCTTGTTCC TCGTTTGAAC GCCCCTGCAG ACCGTTCACC TTCTCCAGGA CCTTC [585]
Florida  CTTTATGGCA TTCTTGTTCC TCGTTTGAAC GCCCCTGCAG ACCGTTCACC TTCTCCAGGA CCTTC [585]
Pakistan CTTTATGGCA TTCTTGTTCC TCGTTTGAAC GCCCCTGCAG ACCGTTCACC TTCTCCAGGA CCTTC [585]
Arizona  CTTTATGGCA TTCTTGTTCC TCGTTTGAAC GCCCCTGCAG ACCGTTCACC TTCTCCAGGA CCTTC [585]
CRF-HI   CTTTATGGCA TTCTTGTTCC TCGTTTGAAC GCCCCTGCAG ACCGTTCACC TTCTCCAGGA CCTTC [585]

CRF-CA   TACTGCATAT CGCTATCGTG GCGAGGAAAA CCCAAAATAT GGACCTAAAA AA-GCAGTGC ATCCG [650]
Florida  TACTGCATAT CGCTATCGTG GCGAGGAAAA CCCAAAATAT GGACCTAAAA AA-GCAGTGC ATCCG [650]
Pakistan TACTGCATAT CGCTATCGTG GCGAGGAAAA CCCAAAATAT GGACCTAAAA AA-GCAGTGC ATCCG [650]
Arizona  TACTGCATAT CGCTATCGTG GCGAGGAAAA CCCAAAATGT GGACCTAAAA AAACAAGGGA TTCCG [650]
CRF-HI   TACTGCATAT CGCTATCGTG GCGAGGAAAA CCCAAAATGT GGACCTAAAA AAACCATGGC TTCCG [650]

CRF-CA   TTGGGGGGAA GGCTTAGCGG T [671]
Florida  TTGGGGGGAA GGCTTAGCGG T [671]
Pakistan TTGGGGGGAA GGCTTAGCGG T [671]
Arizona  TGGGGGGAA- ---------- - [671]
CRF-HI   TTGGGGGAA- ---------- - [671]
```

Fig. S1. Alignment of the sequences of the ENS PCR products shown in Fig. 2. Sequences were aligned using ClustalW and mismatched nucleotides are shaded.

Fig. S2

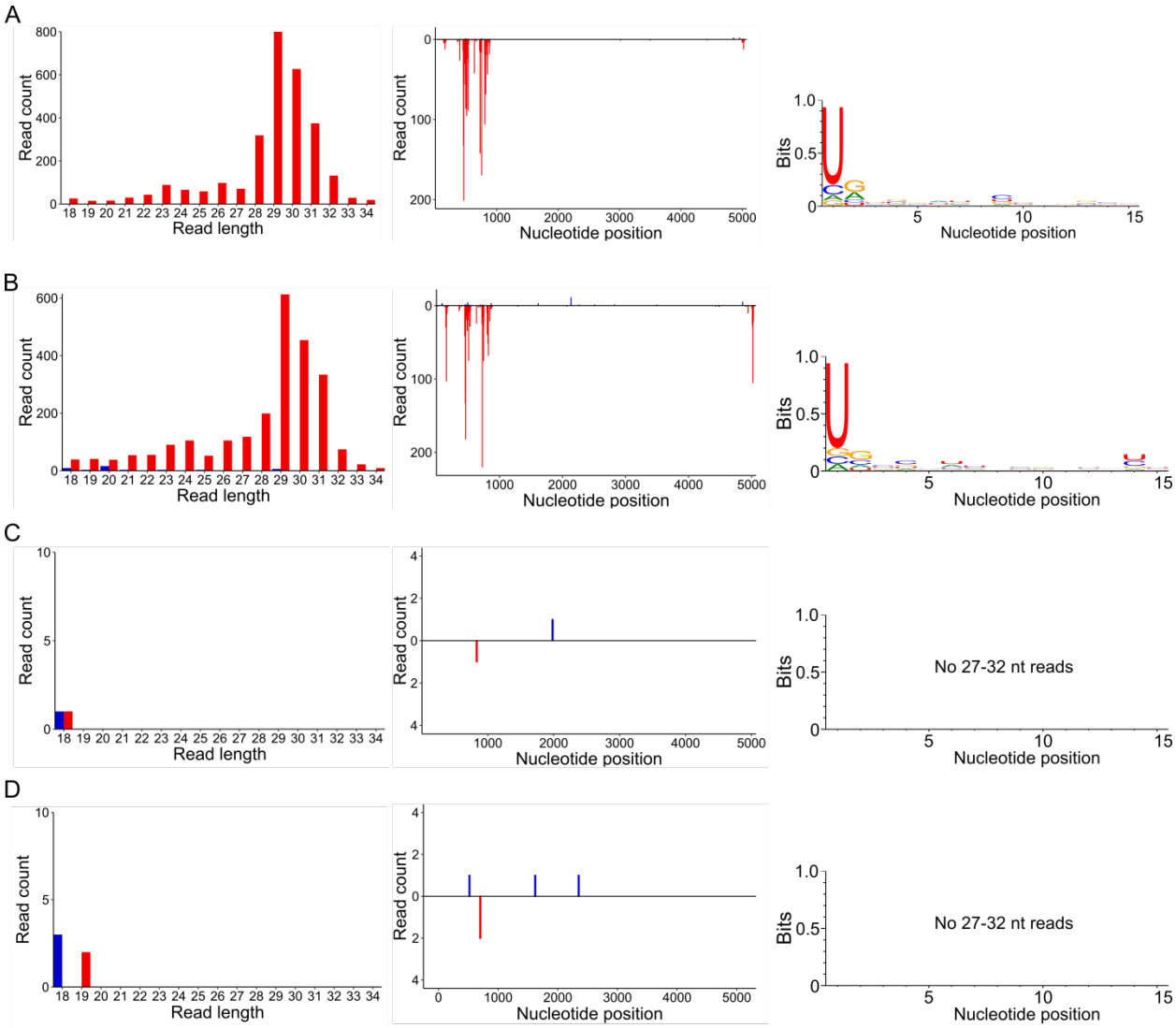

Fig. S2. (A-D) Left: Length distribution of all sRNAs from various *D. citri* populations mapped to the DcDV genome. Red = antisense, blue = sense. Middle: Positions of all sRNAs from various *D. citri* populations mapped to the DcDV genome. sRNAs are shown as mapped to the genomic strand containing the coding sequence for the NS proteins. Red = antisense sRNAs, blue = sense sRNAs. Right: Sequence logo of 27-32 nt sRNAs shown in the left and middle panels. sRNAs were purified from field-collected insects from China (GenBank accession no. SRX1164134)(A), the US state of Florida (GenBank accession no. SRX1164135) (B), Brazil (GenBank accession no. SRX1164127)(C), or laboratory reared insects from CRF-Uru (D). Sequence data for (A-C) are described in (25,26).

Fig. S3

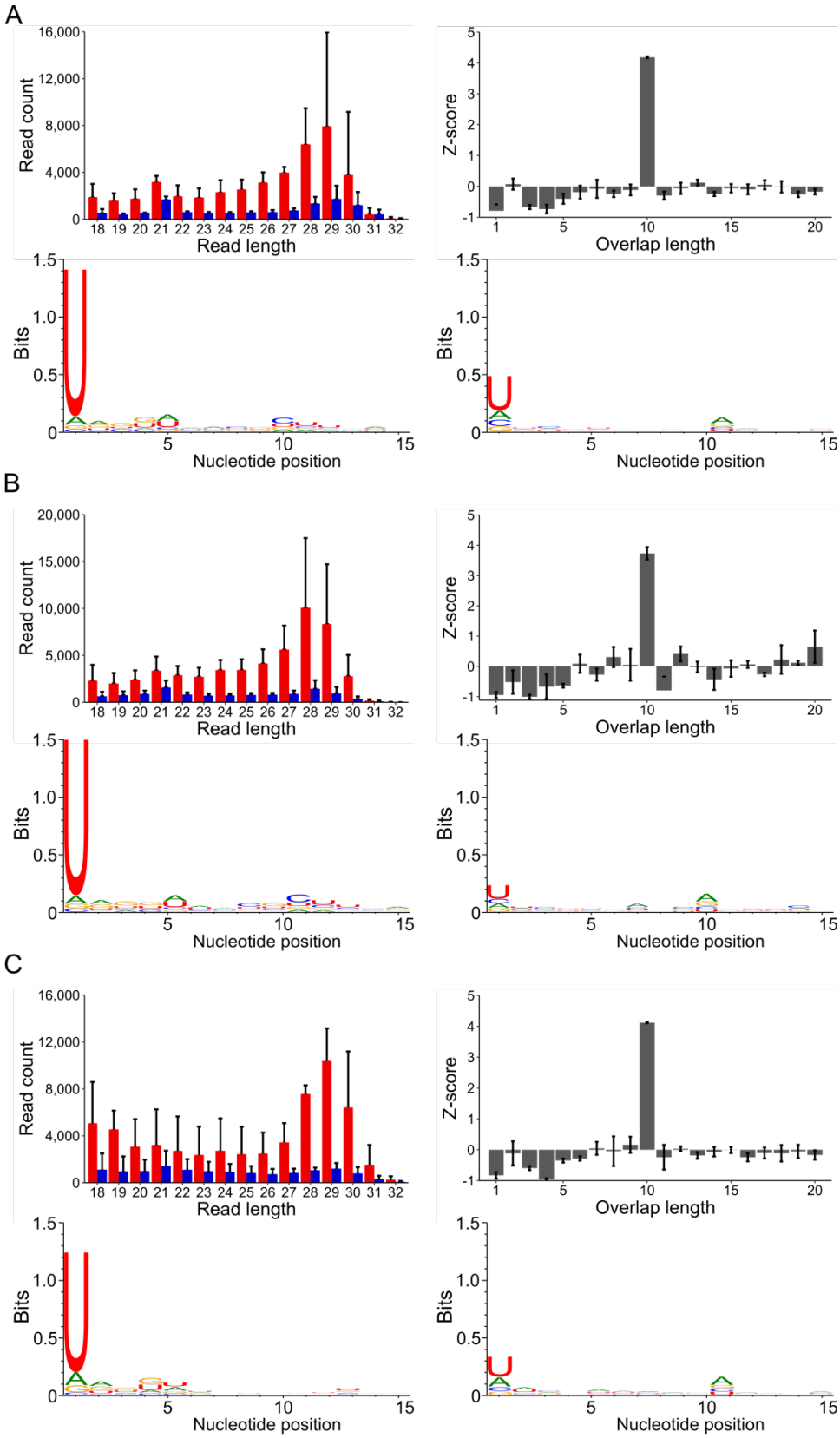
A
Read count
Read length
Z-score
Overlap length
Bits
Nucleotide position
B
Read count
Read length
Z-score
Overlap length
Bits
Nucleotide position
C
Read count
Read length
Z-score
Overlap length
Bits
Nucleotide position

Fig. S3 continued

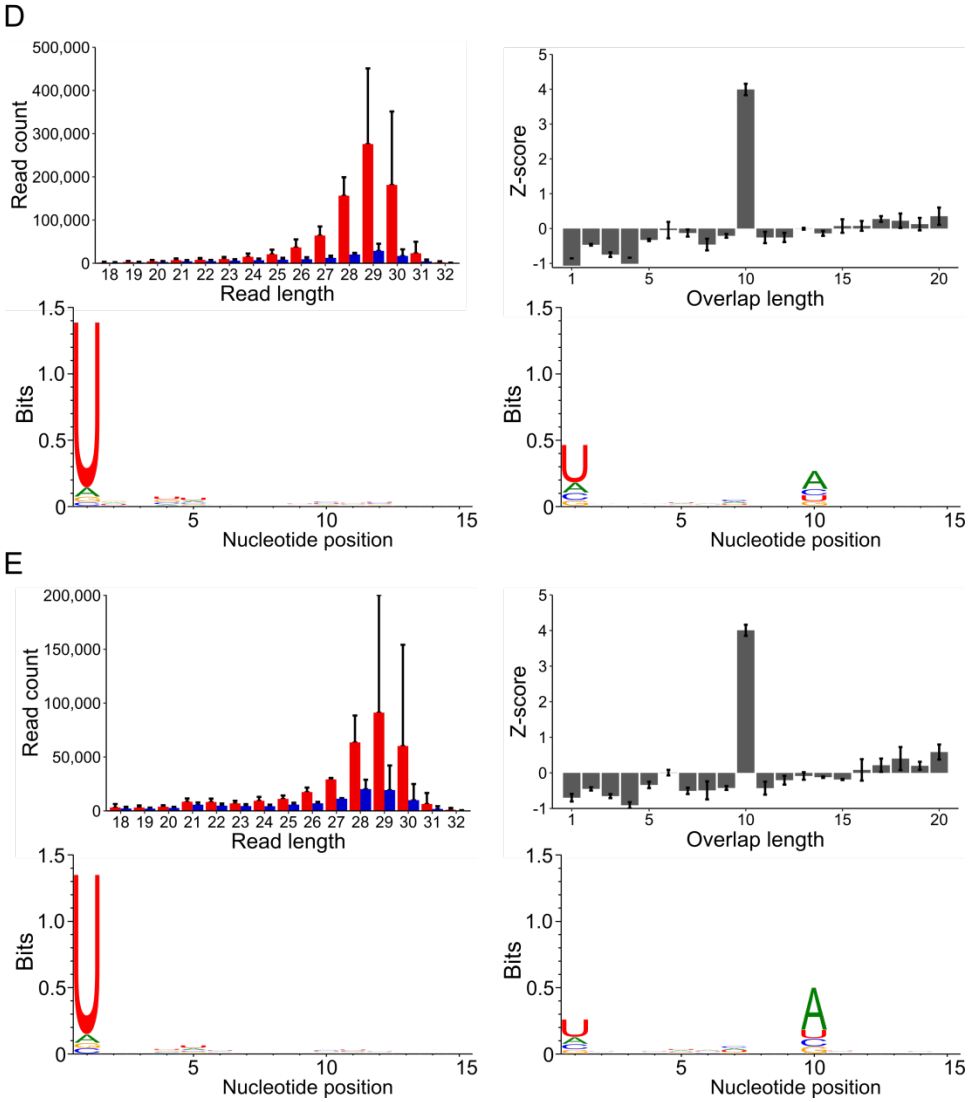

Fig. S3. (A-E) Analysis of sRNAs from dissected CRF-CA *D. citri* tissues. Figures indicate mapping statistics for sRNAs mapping to all TEs identified in the *D. citri* genome. (A) sRNAs from three pools of 200 *D. citri* guts. (B) sRNAs from three pools of 200 *D. citri* heads. (C) sRNAs from three pools of hemolymph from 100 *D. citri* each. (D) sRNAs from three pools of 100 *D. citri* ovaries. (E) sRNAs from three pools of 100 *D. citri* testis. Upper left panels: length distribution of sRNAs mapping to TEs. Red = antisense, blue = sense. Read counts are an average of three independent libraries. Error bars indicate standard deviation. Upper right panels: Z-scores for the indicated overlap distances between the 5' ends of complementary 27-32 nt sRNAs. Z-scores are an average of three independent libraries. Errors bars indicate the standard deviation. Lower panels: Sequence logos for 27-32 nt sRNAs mapping to TEs. Lower left = antisense, Lower right = sense. Data represents three pooled libraries.

1281 **Fig. S4**
1282

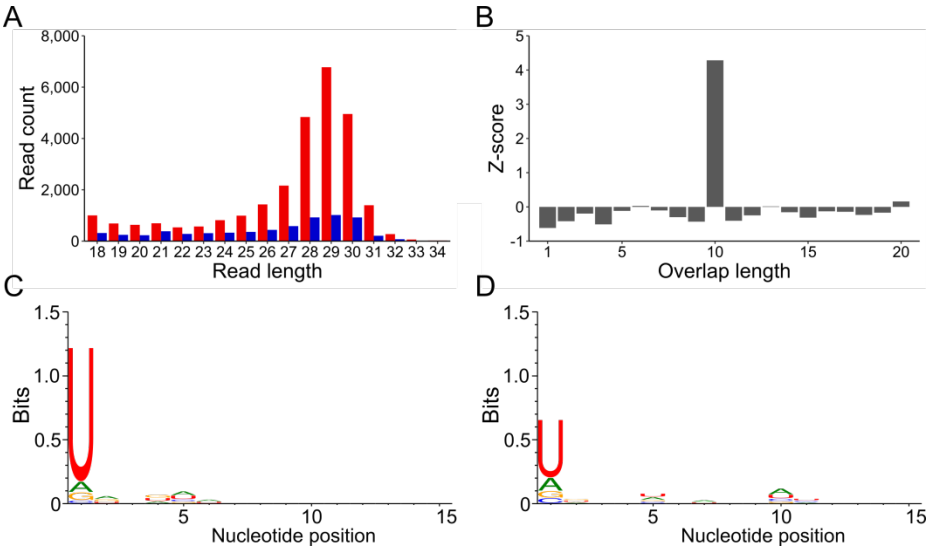

1283
1284
1285 **Fig. S3.** (A-E) Analysis of sRNAs from CRF-Uru *D. citri*. Figures indicate mapping statistics for
1286 sRNAs mapping to all TEs identified in the *D. citri* genome. (A) length distribution of sRNAs
1287 mapping to TEs. Red = antisense, blue = sense. (B) Z-scores for the indicated overlap distances
1288 between the 5' ends of complementary 27-32 nt sRNAs. (C & D) Sequence logos for 27-32 nt
1289 sRNAs mapping to TEs. (C) Antisense sRNAs. (D) Sense sRNAs.
1290
1291
1292
1293
1294
1295
1296
1297
1298
1299
1300
1301
1302
1303
1304
1305
1306
1307
1308
1309
1310
1311
1312
1313

Fig. S5

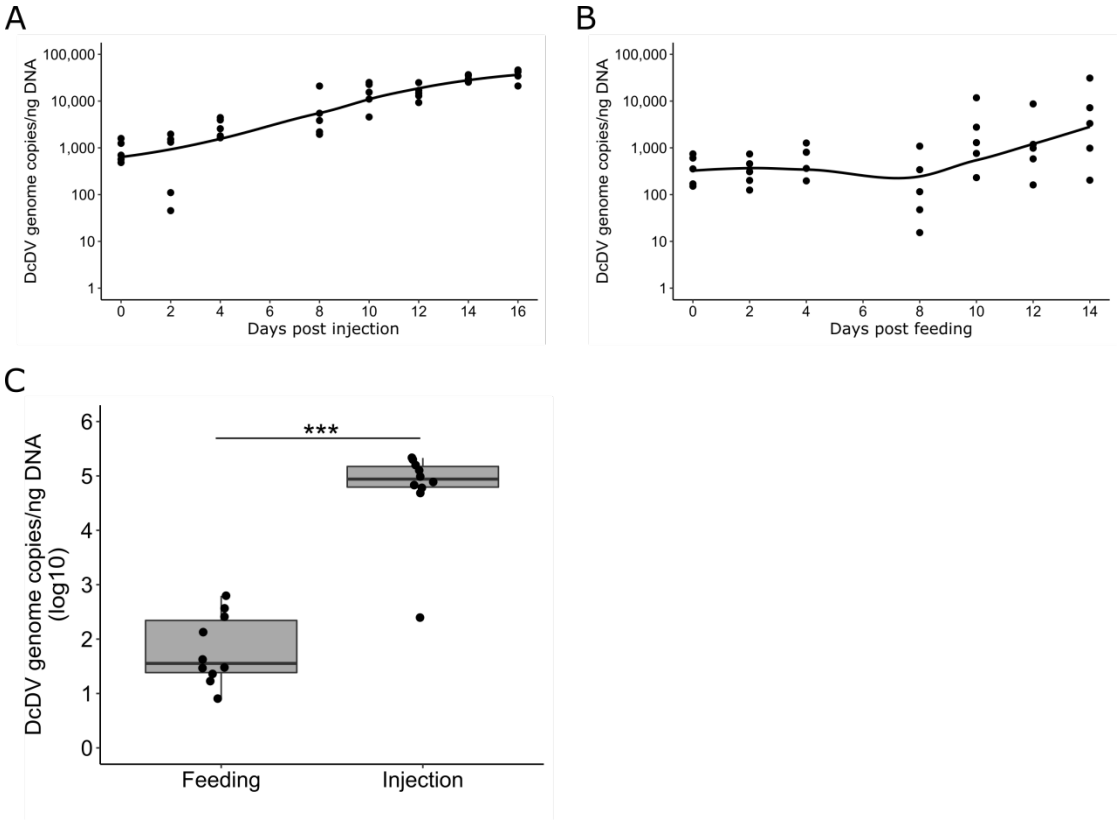

Fig. S4. (A) Titer of DcDV following intrathoracic injection of virions into uninfected *D. citri* insects from CRF-Uru. Each data point represents three pooled insects (n=5). The curve was smoothed using loess regression. (B) Titer of DcDV following feeding of virions to uninfected *D. citri* insects from CRF-Uru. Virions present in a 15% sucrose artificial diet solution were acquired by *D. citri* for 96 hours by membrane feeding. After the feeding period, insects were moved to *Citrus macrophylla* plants and this represents day 0 post feeding. Each data point represents three pooled insects (n=5). The curve was smoothed using loess regression. (C) Titer of DcDV in F1 progeny of the insects shown in (A), designated by injection, and (B), designated by Feeding. n=10 individual insects. Individual insects were collected on the day of emergence to adulthood.

1339 **Fig. S6**
1340
1341

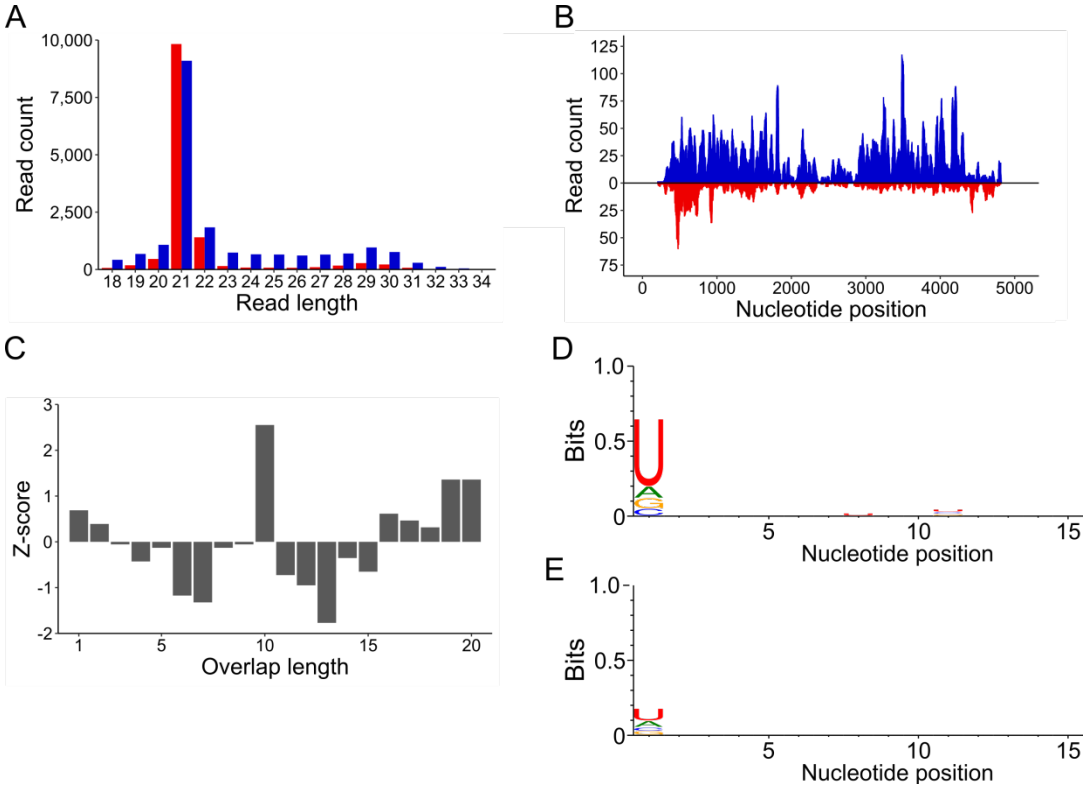

1342
1343

1344 **Fig. S6.** DcDV is targeted by ping-pong-dependent vpiRNAs in DcDV-infected *D. citri* insects
1345 from CRF-Uru. sRNAs were purified from the progeny of CRF-Uru *D. citri* that had been
1346 infected with DcDV by intrathoracic injection (see Fig. S5a & c). (A) Length distribution of
1347 sRNAs mapping to the DcDV genome in DcDV-infected *D. citri* insects from CRF-Uru. To
1348 account for the bidirectional transcription strategy of DcDV, sRNA mapping polarity was
1349 assigned from mapping location based on the start and stop positions of the canonical DcDV
1350 transcripts. Red = antisense sRNAs, blue = sense sRNAs. (B) Positions of 27-32 nt sRNAs
1351 shown in (A). Red = antisense sRNAs, blue = sense sRNAs. (C) Z-scores for the indicated
1352 overlap distances between the 5' ends of complementary 27-32 nt sRNAs shown in (A). (D & E)
1353 Sequence logos for the 27-32 nt sRNAs shown in (A). Sequence logos for antisense sRNAs (D)
1354 or sense sRNAs (E) are shown.
1355
1356
1357
1358
1359
1360
1361
1362
1363
1364

1365 **Fig. S7**

1366

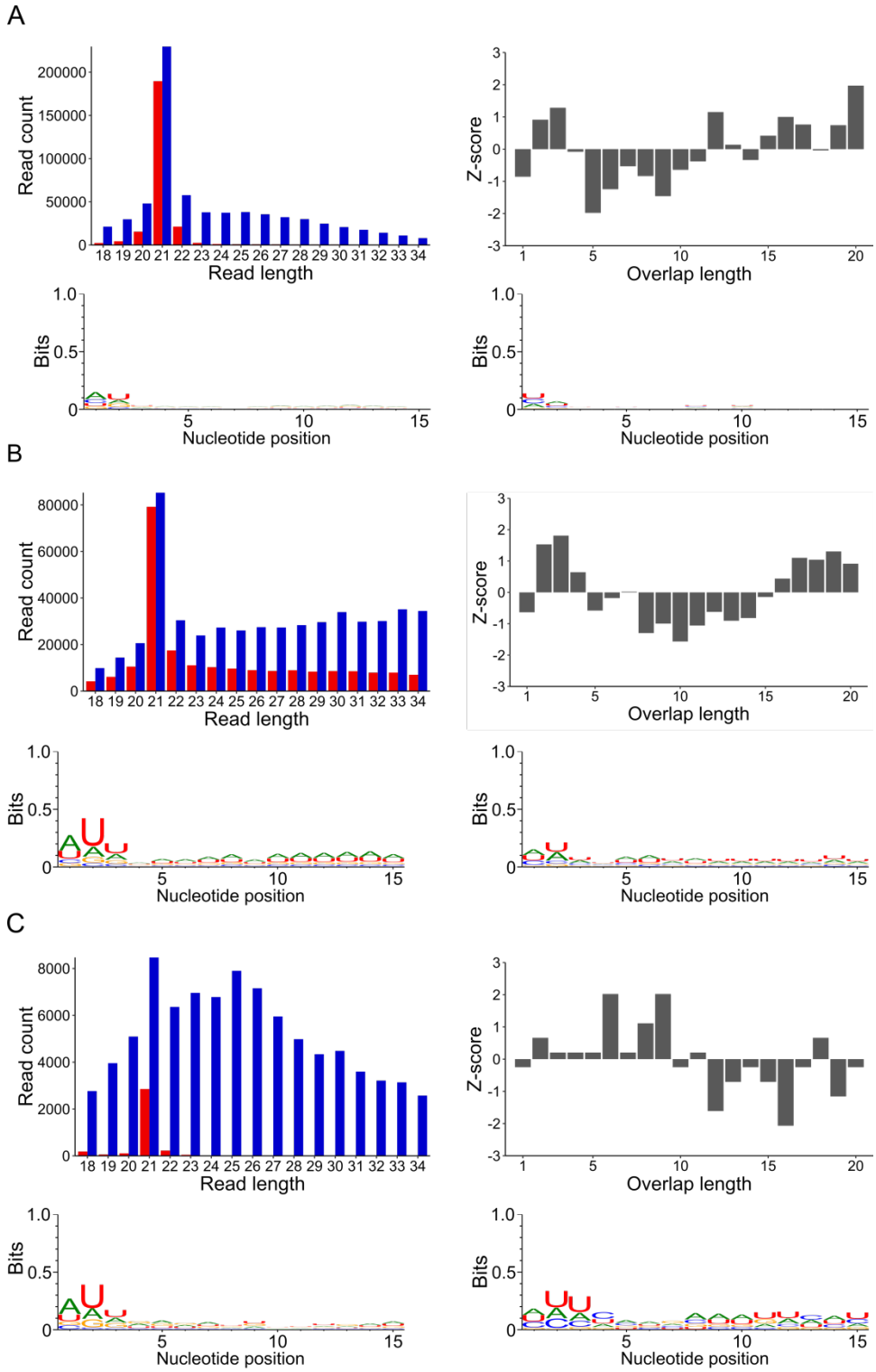

1367
1368
1369
1370

Fig. S7 continued

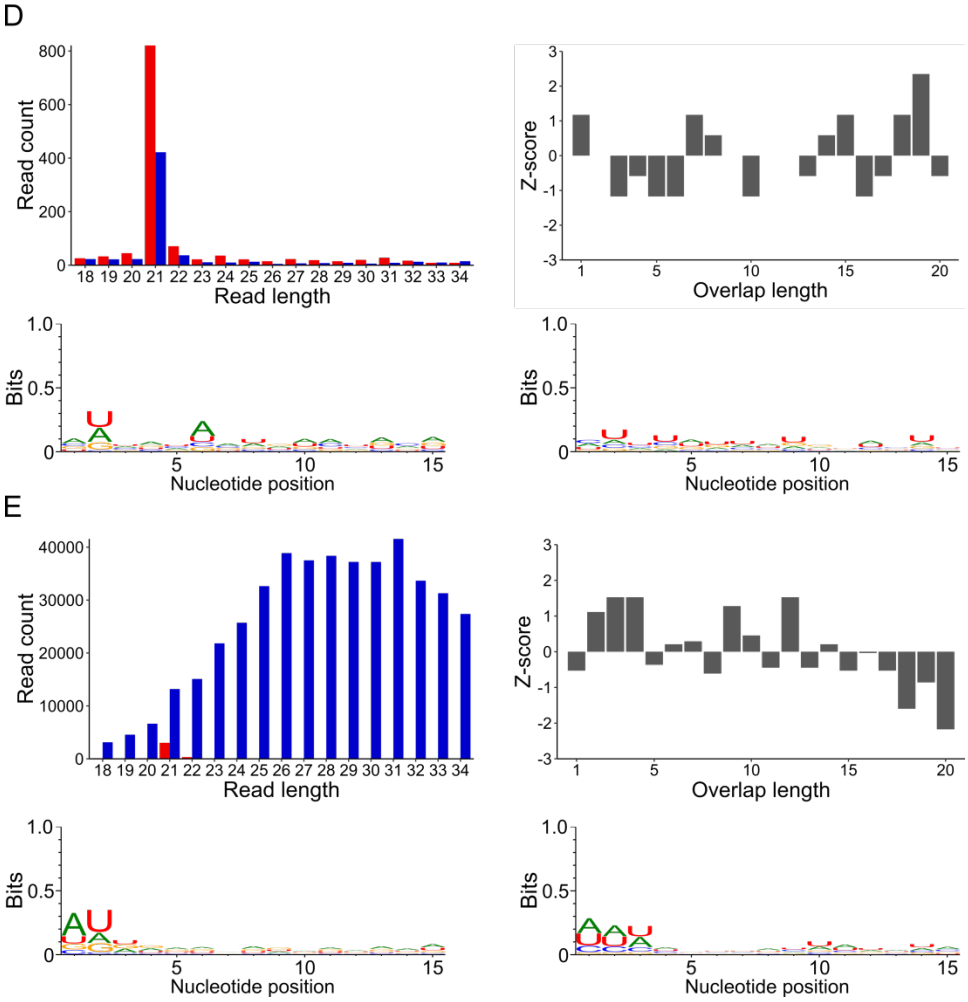

Fig. S7. (A-E) Analysis of sRNAs from various field-collected *D. citri* populations infected with one or more *D. citri*-specific viruses. (A) *D. citri* from the US state of Florida infected with Diaphorina citri flavi-like virus (sRNA GenBank accession no. SRX1164135, viral genome GenBank accession no. NC_030453.1). (B) *D. citri* from China infected with Diaphorina citri reovirus (sRNA GenBank accession no. SRX1164134, viral genome GenBank accession no.'s KT698830.1, KT698831.1, KT698832.1, KT698833.1, KT698834.1, KT698836.1). (C) *D. citri* from China infected with Diaphorina citri picorna-like virus (sRNA GenBank accession no. SRX1164134, viral genome GenBank accession no. KT698837.1). (D) *D. citri* from China infected with Diaphorina citri bunyavirus (sRNA GenBank accession no. SRX1164134, viral genome GenBank accession no.'s KT698825.1, KT698824.1, KT698823.1). (E) *D. citri* from Brazil infected with Diaphorina citri picorna-like virus (sRNA GenBank accession no. SRX1164127, viral genome GenBank accession no. KT698837.1). Upper left panels: length distribution of sRNAs mapped to the various viral genomes. Red = antisense, blue = sense. Upper right panels: Z-scores for the indicated overlap distances between the 5' ends of complementary 27-32 nt sRNAs mapping to opposite strands of the various viral genomes.

1390 Sequence data are described in (25,26). Lower panels: Sequence logos for 27-32 nt sRNAs
1391 mapping to the various viral genomes. Lower left = antisense, Lower right = sense.
1392
1393
1394
1395
1396
1397
1398
1399
1400
1401
1402
1403
1404
1405
1406
1407
1408
1409
1410
1411
1412
1413
1414
1415
1416
1417
1418
1419
1420
1421
1422
1423
1424
1425
1426
1427
1428
1429
1430
1431
1432
1433
1434
1435

Fig. S8

```
CrPV-DcDNV (1352-1473)   CTTTTGATGA GTGGTgatgt cgaatctaat cctggtcctg CAGACCGTTC ACCTTCTCCA   [ 60]
DcDNV (803-859)          ---------- ---------- ---------- ---------g CAGACCGTTC ACCTTCTCCA   [ 60]
NW_007380266 (8062-8118) ---------- ---------- ---------- ---------g CAGACCGTTC ACCTTCTCCA   [ 60]

CrPV (1171-1224)         CTTTTGATGA GTGGTgatgt cgaatctaat cctggtcctg ---------- ----------   [ 60]

CrPV-DcDNV (1352-1473)   GGACCTTCTA CTGCATATCG CTATTGTAGC GAGGAAgatg tcgaatctaa tcctggtcct  [ 120]
DcDNV (803-859)          GGACCTTCTA CTGCATATCG CTATTGTAGC GAGGAA---- ---------- ----------  [ 120]
NW_007380266 (8062-8118) GGACCTTCTA CTGCATATCG CTATCGTGGC GAGGAA---- ---------- ----------  [ 120]

CrPV (1171-1224)         ---------- ---------- ---------- ---------- ---------- ----------  [ 120]

CrPV-DcDNV (1171-1473)   gTGCAATCGC GCCCC [135]
DcDNV (803-859)          ---------- ----- [135]
NW_007380266 (8062-8118) ---------- ----- [135]
CrPV (1171-1224)         -TGCAATCGC GCCCC [135]
```

Fig. 8. Alignment of a portion of the CrPV-DcDV genome, the recombinant DcDV sequence present within CrPV-DcDV, the region of ENS corresponding to the recombinant DcDV sequence present within CrPV-DcDV (represented by the GenBank accession no. of *D. citri* genomic scaffold 2850, NW_007380266), and a portion of the wild-type CrPV sequence. Numbers in parentheses indicate the nucleotide positions of the sequence shown. The CrPV 1A cleavage site is shown in lowercase letters. The recombinant DcDV sequence present within CrPV-DcDV and the corresponding region of ENS are shown in italics.

1475 **Fig. S9**
1476

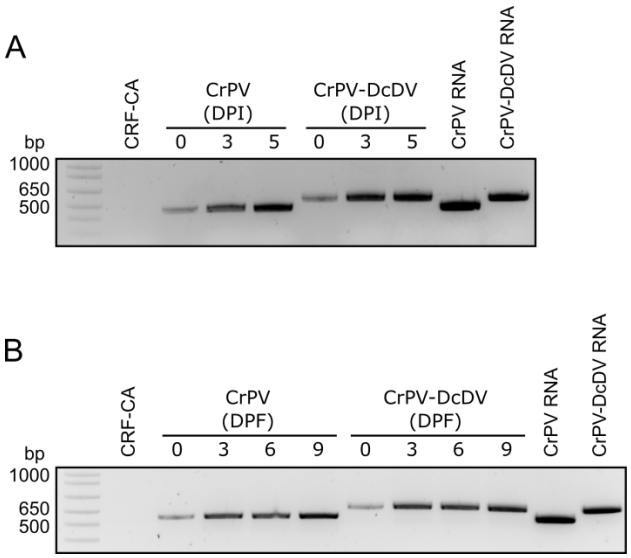

1477
1478
1479 **Fig. S9.** RT-PCR products produced using primers flanking the site into which recombinant
1480 DcDV sequence was inserted in CrPV-DcDV (primers 15 and 16). RNA from all biological
1481 replicates from each day shown in Fig. 4.6a (A) or Fig. 4.7a (B) was pooled and used as
1482 templates for RT-PCR. RNA from CRF-CA *D. citri* was used as a negative control. *In vitro*
1483 transcribed wild-type CrPV or CrPV-DcDV RNA was used as a positive control. DPI = days
1484 post injection. DPF = days post feeding.
1485
1486
1487
1488
1489
1490
1491
1492
1493
1494
1495
1496
1497
1498
1499
1500
1501
1502
1503
1504
1505
1506
1507

1508 **Fig. S10**
1509

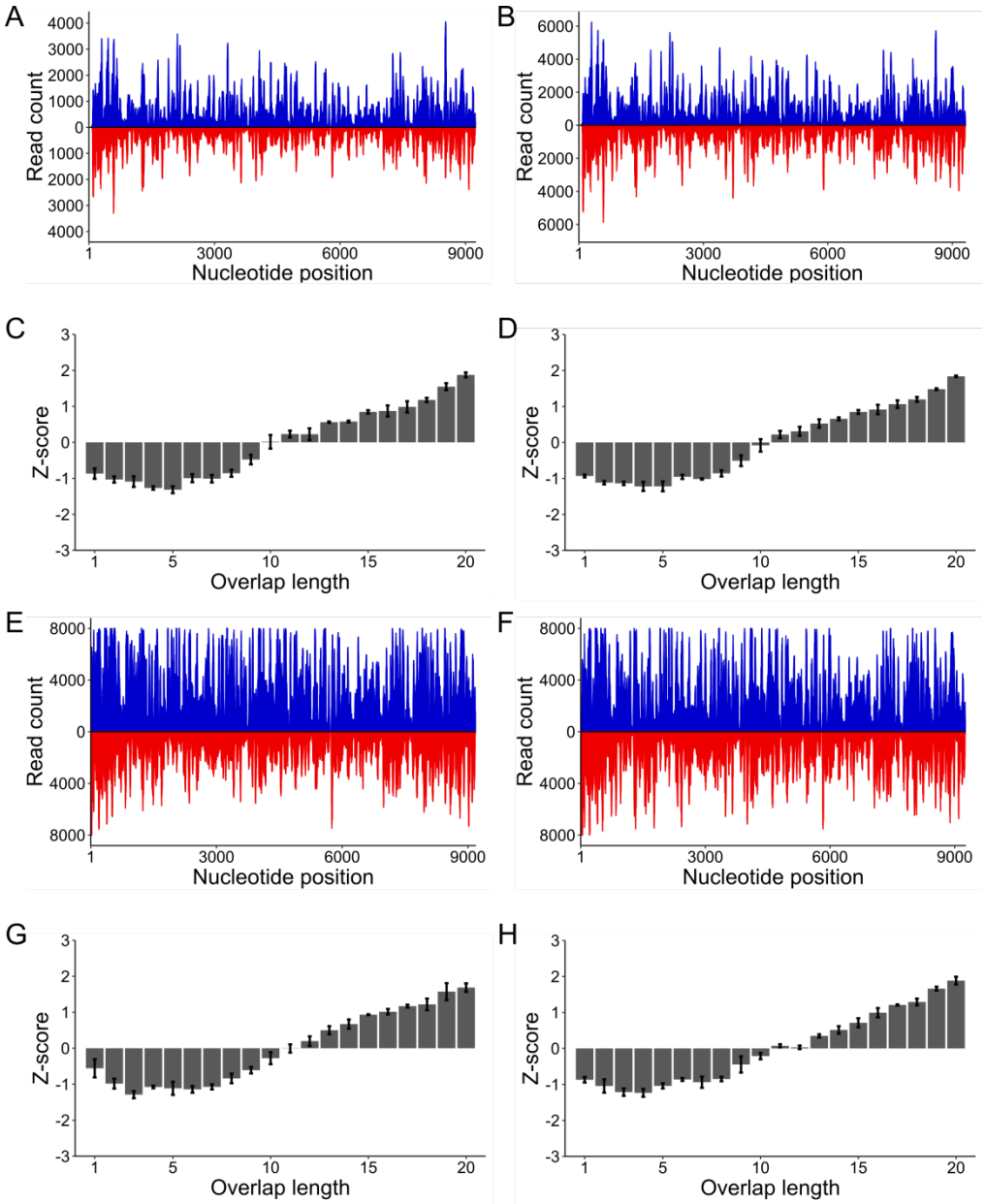

1510
1511 **Fig. S10.** (A & B) Positions of 21 nt sRNAs mapping to the wild-type CrPV genome (A) or the
1512 CrPV-DcDV genome (B) during infection of CRF-CA *D. citri* initiated by intrathoracic injection
1513 of virions. Red = antisense sRNAs, blue = sense sRNAs. Reads counts are an average of three
1514 independent libraries. (C & D) Z-scores for the indicated overlap distances between the 5' ends
1515 of complementary 27-32 nt sRNAs mapping to opposite strands of the wild-type CrPV genome
1516 (C) or the non-recombinant portion of the CrPV-DcDV genome (D) during infection of CRF-CA
1517 *D. citri* initiated by intrathoracic injection of virions. Z-scores represent the average of three
1518 independent libraries. Error bars indicate standard deviation. (E & F) Positions of 21 nt sRNAs
1519 mapping to the wild-type CrPV genome (E) or the CrPV-DcDV genome (F) during infection of
1520 CRF-CA *D. citri* initiated by oral acquisition of virions. Red = antisense sRNAs, blue = sense
1521 sRNAs. Reads counts are an average of three independent libraries. (G & H) Z-scores for the

1522 indicated overlap distances between the 5' ends of complementary 27-32 nt sRNAs mapping to
1523 opposite strands of the wild-type CrPV genome (G) or the non-recombinant portion of the CrPV-
1524 DcDV genome (H) during infection of CRF-CA *D. citri* initiated by oral acquisition of virions.
1525 Z-scores represent the average of three independent libraries. Error bars indicate standard
1526 deviation.
1527
1528
1529
1530
1531
1532
1533
1534
1535
1536
1537
1538
1539
1540
1541
1542
1543
1544
1545
1546
1547
1548
1549
1550
1551
1552
1553
1554
1555
1556
1557
1558
1559
1560
1561
1562
1563
1564
1565
1566
1567

1568 **Table S1**

Primer #	Sequence (5’ → 3’)
1	GGGAAAATCGGTCTCATGCTGCTGTT
2	AAATTGGAGTTAGAAGCTAAAGTTACC
3	TGTAACTTTAGTATGGACTGTTCAGC
4	TTCTTTCACTCCAAACTCTTTCTAGAATGC
5	CCTCTGAGTTCTGCTCCAGC
6	AACAGCAGCATGAGACCGATTTTCCC
7	TGACACCGCTAAGCCTTCC
8	ACACTTTTTTAAAAGCGATAAGTTGTC
9	CCCTGGACTTTGAACAGGAA
10	CATTTGCGGTGAACGATTCC
11	CCAGAACATCGATATGGATCAAC
12	TTGAATTTGGGCTGTTAGTGTC
13	GTGCAATCGCGCCCCGTATATG
14	AGGACCAGGATTAGATTCGACATCAC
15	CCAGAACATCGATATGGATCAAC
16	/phos/TTGAATTTGGGCTGTTAGTGTC†
17	/phos/AGATTCGACATCTTCCTCGCTACAATAGCG†
18	AATCCTGGTCCTGTGCAATCGCGCC
19	GGAAGAATGGCGAATTTTGA
20	CTCGGGAAAGATCCATTTCA
21	TCGTGACATCAAGGAGAAGCTGTGC
22	TTGACCGTCGGGAAGTTCGTAGGAT
23	TATAAATAGAGGCGTTTCTGTTGTG
24	TAATACGACTCACTATAGGGCGATCGCCAAGCCTTCC
25	TAATACGACTCACTATAGGGTATAAATAGAGGCGTTTCTGTTGTG
26	CGATCGCCAAGCCTTCC
27	TAATACGACTCACTATAGGGTGACACCGCTAAGCCTTCC

1569 † /phos/ indicates 5’ phosphorylation
1570
1571
1572
1573